Spring 2022

An Analysis of Wet Bulb Globe Temperature Estimation Methods and Microclimate Heat Variability in Columbia, South Carolina

Stafford Mullin

AN ANALYSIS OF WET BULB GLOBE TEMPERATURE ESTIMATION METHODS AND MICROCLIMATE HEAT VARIABILITY IN COLUMBIA, SOUTH CAROLINA

by

Stafford Mullin

Bachelor of Arts
University of South Carolina, 2020

Submitted in Partial Fulfillment of the Requirements

For the Degree of Master of Science in

Geography

College of Arts and Sciences

University of South Carolina

2022

Accepted by:

Greg Carbone, Director of Thesis

April Hiscox, Reader

Kirstin Dow, Reader

Tracey L. Weldon, Interim Vice Provost and Dean of the Graduate School

ACKNOWLEDGEMENTS

I am deeply grateful for Dr. Greg Carbone for his substantial guidance and support throughout the process of my master's degree and this thesis research. Truthfully this work would not have been possible without his help every step of the way. I would also like to thank Dr. April Hiscox and Dr. Kirstin Dow for their feedback and suggestions on this work, every day I feel lucky to have a committee that believed in and supported me when I needed it. I would also like to thank my fellow graduate students and good friends, Lily, Chris, Margot, Patrick, Grant, Derek, Andrew, and Leah. You've all been the best emotional cheerleaders I could ask for and I cherish our time spent together. Lastly, thank you to my family for their constant encouragement throughout the past two years.

ABSTRACT

Extreme heat is the leading cause of weather-related deaths in the United States and poses major health risks in the wake of rising global average temperatures. Wet bulb globe temperature (WBGT) is a holistic measure of human heat stress, but is not feasible to implement in most settings because the equipment is expensive and troublesome to operate. This research evaluates the performance of WBGT estimation methods using more standard meteorological variables, measured in-situ and a local National Weather Service Automated Surface Observing Station, and examines how WBGT and its components vary across two distinct microclimates in Columbia, SC. Results indicate that the Stull and Black Globe Regression (BGR) method may be a reasonable proxy for WBGT, particularly when a localized data source is available, but this method likely underestimates heat risk. Alternatively, the Australian Bureau of Meteorology (ABM) method tends to overpredict WBGT but is the most convenient and accessible monitoring method because its only data inputs, temperature and relative humidity, are more readily available. Results also demonstrate meaningful differences in heat characteristics, such as temperature, humidity, and solar radiation, observed on a brick and a grass measurement site. These differences shed light on diurnal fluctuations in heat characteristics including elevated warming over the brick surface at nighttime, and higher moisture levels over the grass site leading to more oppressive daytime heat.

TABLE OF CONTENTS

LIST OF TABLES

LIST OF FIGURES

LIST OF SYMBOLS

T_a	Ambient air temperature
T_{wb}	Wet bulb temperature
T_{bg}	Black Globe Temperature

LIST OF ABBREVIATIONS

ANOVA ..... Analysis of Variance

ASOS ..... Automated Surface Observation System

BGR ..... Black Globe Regression

COOP ..... Cooperative Observer Program

HI ..... Heat Index

KCUB ..... Jim Hamilton L B Owens Airport

MAE ..... Mean Absolute Error

MBE ..... Mean Bias Error

NWS ..... National Weather Service

RMSE ..... Root Mean Square Error

UHI ..... Urban Heat Island

VIF ..... Variance Inflation Factor

WBGT ..... Wet Bulb Globe Temperature

WBR ..... Wet Bulb Regression

W/m^2 ..... Watts per Square meter

CHAPTER 1

INTRODUCTION

The public health threats posed by extreme heat are made clear by associations between daily temperatures and mortality (Kalkstein & Davis, 1989), as well as excess deaths (Whitman et al., 1997) and emergency room admissions (Fuhrmann et al., 2016). Extreme heat is recognized as the predominant weather-related cause of death in the United States (NOAA, 2020). This health hazard is becoming particularly noteworthy in the wake of global climate change and growing atmospheric greenhouse gas concentrations. Future projections indicate the emergence of heat and humidity conditions approaching human survivability thresholds (Raymond et al., 2020), as well as the possibility for heatwaves of greater intensity and duration (Meehl & Tebaldi, 2004). Some analyses suggest under current greenhouse gas emissions scenarios, three fourths Earth's population could be exposed to deadly environmental conditions for at least 20 days per year during the next century (Mora et al., 2017).

Given the changing character of extreme heat events and their known detriment to human health, further evaluation of extreme heat will be paramount in the coming decades, especially for at-risk populations. One adaptive avenue for minimizing the harmful effects of heat exposure is through proper monitoring of dangerous exposure levels, especially for subpopulations who spend a significant amount of time working or performing strenuous activities outdoors. Historically, the wet bulb globe temperature (WBGT) thermometer has been the gold standard heat stress index to monitor unsafe

weather conditions in groups who perform strenuous activities in outdoor environments, such as Army and Marine Corps recruits, athletes, and occupational groups. Through the integration of ambient air temperature, humidity, wind speed, and solar radiation, WBGT provides a comprehensive measurement of thermal comfort to protect individuals from performing in unsafe conditions, and accordingly, is the recommended method by the Occupational Safety and Health Administration (OSHA) for monitoring heat in the workplace.

According to the Fourth National Climate Assessment, industries could lose nearly 2 billion labor hours annually by the end of the century (Ebi et al., 2018) due to unsafe working conditions, with roughly one third of this lost productivity concentrated in the southeastern United States (Carter et al., 2018). Thus, accurately monitoring environmental heat conditions for outdoor laborers is critical. Despite its merits as a holistic heat exposure metric, WBGT instrumentation is not feasible in most workplaces due to expensive equipment costs and high maintenance needs. Appropriately, estimation techniques for WBGT and its components have emerged as substitutes since they tend to use more common meteorological variables, thus enhancing the measures accessibility. Such approximation techniques and proxy measurements require further evaluation for their efficacy and ease of use, with the goal of protecting the health of outdoor workers and preventing lost productivity in the workplace.

1.1 PURPOSE AND OBJECTIVES

The purpose of this research is twofold; to evaluate the efficacy and performance of WBGT estimation methods against ground truth measurements, and to understand how WBGT varies across two microclimate environments in Columbia, SC.

Building upon previous efforts to evaluate such estimation methods, WBGT is estimated using the Australian Bureau of Meteorology (ABM) method, and the Stull and Hajizadeh regression methods. The latter two methods estimate wet bulb and black globe temperature, which are essential components of WBGT. Data from a variety of sources is be used to perform the estimation, including localized data recorded at the WBGT measurement site, contrasted with measurements from local airport weather stations. The purpose of comparing model outputs from in-situ data versus airport weather station data, is to determine if local data inputs improve model performance by better accounting for microclimate variability. The modeled estimates will be validated against WBGT measurements derived from a Kestrel 5400 Heat Stress tracker. The overarching goal of this phase of the analyses is to evaluate if WBGT can be estimated using the selected modeling techniques, and if these methods may serve as reasonable substitutes for real time monitoring in workplaces. Specifically, objectives are to 1) quantify how the estimated WBGT methods perform compared to observed WBGT measurements, 2) evaluate whether the inclusion of localized data (compared to airport weather station data) improves the estimations, and 3) investigate times of day and weather conditions in which the estimates perform most accurately.

Considering the limitations associated with on-site WBGT monitoring, understanding how much WBGT varies across different microenvironments may better inform monitoring practices across a diverse set of workplaces. Accordingly, the second facet of the research is intended to evaluate how WBGT differs across a brick and a grass surface at the COOP site in Columbia, SC by evaluating hourly difference scores between the two sites.

1.2 RESEARCH QUESTIONS

To address these objectives, the following research questions direct the research:

1) Can WBGT be reasonably estimated using the Australian Bureau of Meteorology (ABM), and the Stull & Black Globe Regression (BGR) methods?
2) Does the integration of meteorological data from localized data sources, compared to airport weather station data improve model accuracy, and are there particular times of day and weather conditions in which the estimation methods perform more accurately?
3) How does WBGT intensity vary across the grass versus brick environments?

In accordance with prior research quantifying the accuracy of ABM, it is hypothesized that the ABM model will perform reasonably well midday and less accurately during morning and afternoon hours when sun angle is lower. Additionally, it is hypothesized that WBGT using parameters derived from the (Stull, 2011) equation and BGR Method (Hajizadeh et al., 2017) will be closer to WBGT values measured by a Kestrel 5400 instrument. Consistent with the findings of Carter et al. (2020), it is also hypothesized that the integration of atmospheric data recorded at the WBGT measurement site will improve model performance compared more distant airport weather station data.

It has also been theorized that WBGT values across the brick and grass surfaces at the weather station in Columbia will experience little variability. However, it is theorized that the brick surface will retain heat through nighttime hours, resulting in slightly elevated WBGT values in the early morning hours (8:00 AM – 11:00 AM), and will become comparable to WBGT measurements on the grass surface during the day.

CHAPTER 2

LITERATURE REVIEW

Elevated temperatures are associated with heat related morbidity and mortality, but some individuals are more at risk than others. Broadly, many subgroups have a stake in heat exposure monitoring. This tends to include individuals who are medically susceptible to heat and possess some pre-existing conditions that may aggravate heat related illnesses, as well as individuals who are occupationally exposed to heat due to the nature of their outdoor profession or sport. As such, improvements to WBGT monitoring are advantageous to a wide swath of the population.

2.1 MEDICAL SUSCEPTIBILITY

Epidemiologically, several subgroups experience enhanced medical susceptibility to extreme heat. Older adults (age 65 and older) are disproportionately at risk to heat related health complications (Greenberg et al., 1983). Roughly three-fourths of heat related deaths during the 1995 Heatwave in Chicago, Illinois were comprised of older adults (Whitman et al., 1997). Additionally, older adults tend to be hospitalized or taken to the emergency room at higher rates during heat episodes. This physiological susceptibility is a function of decreased thermoregulatory abilities as well as suppressed cardiovascular function (Kenney et al., 2014). Individuals with pre-existing comorbidities such as cardiovascular diseases, diabetes, and renal diseases also have been tied to increased hospitalization due to heat exposure (Semenza, 1999). Finally, a variety of pregnancy related complications have been associated with heat exposure, such

premature births (Ward et al., 2019) and low birth weights (Bekkar et al., 2020). These epidemiological pathways are not uncommon in the United States. The U.S. is characterized by an aging population, with roughly 50 million individuals over the age of 65 as of 2016 (Roberts et al., n.d.), and roughly 18 million Americans with coronary heart disease (Fryar, 2012). Given that these relatively common conditions are also some of the most prevalent epidemiological drivers of heat related illnesses, real time monitoring of extreme heat and forecasting WBGT would be advantageous to the public.

2.2 VULNERABLE POPULATIONS

In addition to physiological vulnerability, many sub-groups experience increased exposure to hot environmental conditions compared to the average person. Historically, military personnel, athletes, and occupational laborers rely on WBGT monitoring to inform safe training, practice, and workplace conditions. Since these populations tend to perform strenuous or physically demanding activities in outdoor environments, they are particularly at risk to heat illness, thus making proper WBGT monitoring critical. WBGT first emerged in the 1950s (Yaglou and Minard, 1957) in response to high incidence of heat-related illnesses and deaths that plagued United States Military training depots. Exertional heat related illnesses proliferated amongst U.S. Army and Marine Corps recruits, killing nearly 200 Army soldiers, and injuring over 600 trainees at the Parris Island, South Carolina Marine Corps Recruit Depot. By replacing effective temperature with WBGT, properly enforcing WBGT flag protocols, and protecting more vulnerable recruits by prohibiting drilling at hazardous environmental thresholds, incidence of heat illnesses at Parris Island were cut to just under 5 per 10,000 trainees in 1956 (Budd, 2008). Exertional heat related injuries and deaths are entirely preventable by prohibiting

activity during dangerous heat conditions; clearly, the advent of the WBGT monitoring system in the U.S. Military has proven an effective tool for preventing these negative outcomes.

WBGT instrumentation is still used today by the United States Department of Defense but has since been adopted by a variety of other actors who share the same need to monitor heat exposure. WBGT has become especially popular amongst athletic departments and sports medicine professionals. Appropriately, both the National Athletic Trainer's Association as well as the American College of Sports Medicine (1984) recommend WBGT for monitoring unsafe environmental conditions during practices. In practice settings, WBGT provides guidance for modifying activity levels to avoid strenuous workouts during the hottest periods (Figure 2.1), establishing proper breaks for rest and hydration, as well as practice length (Tripp et al., 2020) by designating various heat risk categories. The green, yellow, red, and black flag categories correspond with a particular risk of heat exposure, and recommended activity modifications (Figure 1). Effective WBGT monitoring has become especially crucial for football athletes (A. J. Grundstein et al., 2018), who are notoriously plagued by heat illnesses due to protective gear worn during periods of intense physical exertion.

In addition to military training and athletic settings, WBGT is also an effective tool in occupational and industrial workplaces. It is currently recommended by the Occupational Safety and Health Administration (OSHA), the American Conference of Governmental Industrial Hygienists, as well as the National Institute for Occupational Safety and Health (NOISH) for monitoring of occupational environmental exposure at worksites (Tripp et al., 2020). Many outdoor workers would benefit from WBGT

monitoring, including agricultural workers, construction workers, landscapers, law enforcement, and others. Accordingly, heat exposure has become recognized as a serious occupational hazard (Gubernot et al., 2014) for its potential to cause injury and even fatality on job sites. Literature suggests that migrant farmworkers are particularly vulnerable to heat related illnesses, especially in rural areas (Kovach et al., 2015). Since many farmworkers' workers receive payment based on the volume of crop harvested rather than a set hourly wage, they may be strongly dis-incentivized to take proper rest breaks out of the heat. This may encourage overzealousness at work to maximize pay, making these individuals more susceptible to falling ill (Luque et al., 2019). Additionally, certain occupations such as law enforcement may be required to wear personal protective equipment or body armor uniforms, which could enhance heat exposure symptoms. Such groups ought to take appropriate precautions to avoid heat illness episodes (Lehmacher et al., 2006). Evidently, greater exposure to heat hazards due to more time spent outdoors, compounded with various occupation specific risk factors, brings to light the importance of WBGT monitoring in workplace settings.

WBGT / RISK	IMPACTS	ACTIONS
80-85 F / Low	Body stressed after 45 minutes	Take at least 15 minutes of breaks each hour if working or exercising in direct sunlight, Stay hydrated.
85-88 F / Moderate	Body stressed after 30 minutes. HEAT CRAMPS likely (painful contraction of muscles, weakness)	Take at least 30 minutes of breaks each hour if working or exercising in direct sunlight. Drink ½ to 1 quart of water per hour.
88-90 F / High	Body stressed after 20 minutes. HEAT EXHAUSTION likely (dizziness, nausea, vomiting, headache, fainting, disorientation, weakness)	Take at least 40 minutes of breaks each hour if working or exercising in direct sunlight. Reduce work, exercise intensity. Drink up to 1 quart of water per hour.
> 90 F / Extreme	Body stressed after 15 minutes. HEAT STROKE likely (extremely high body temp, confusion, convulsions, unconsciousness, death)	Take at least 45 minutes of breaks each hour if working or exercising in direct sunlight. Suspend all strenuous outdoor activities. Drink at least 1 quart of water per hour.
Adapted from U.S Army and OSHA guidelines and recommendations		

Figure 2.1 WBGT Heat Categories, source: NWS

2.3 WET BULB GLOBE TEMPERATURE MONITORING

Heat exposure can cause morbidity and mortality in a wide swath of populations and is expected to become more widespread with climate change. A variety of meteorological indicators measure and monitor thermal heat stress. The Wet Bulb Globe Temperature (WBGT) thermometer, represented by Equation [1], is deemed to be one of the most physically accurate indices of thermal heat stress. Its components include natural wet bulb temperature (T_{nwb}), black globe temperature (T_g), and dry bulb temperature (T_{db}). These variables allow for consideration of not only air temperature and humidity, but also wind speed and solar radiation (Yaglou & Minard, 1957). The addition of wind speed and solar radiation effects have a large impact on physiological thermal comfort, making this index more comprehensive compared to other more common measurements such as the Heat Index, that solely relies on temperature and relative humidity.

$$\boldsymbol{WBGT = (0.7 \times T_{wb}) + \left(0.2 \times T_{bg}\right) + (0.1 \times T_a)} \quad \textbf{[1]}$$

The natural wet bulb temperature is the heaviest weighted variable in WBGT, thus emphasizing the critical role of air moisture and air movement in determining thermal comfort. Natural wet bulb temperature is measured with a sling psychrometer, which uses a thermometer fixed with a wet wick on the bulb. When the wet bulb is exposed to naturally moving air in an outdoor environment, it measures the level of evaporative cooling that occurs, which is largely influenced by humidity as well as air movement. Humidity and wind speed are crucial components for predicting heat stress (Budd, 2008), since humans shed heat through evaporative cooling of sweat on the skin. When surrounding air is more moisture laden and stagnant, the evaporation of sweat

becomes less efficient, thus inhibiting the body's ability to affectively shed heat and achieve a desirable level of thermal comfort. Alternatively, drier and faster moving air allows for more efficient perspiration and shedding of metabolic heat. In fact, a breeze of 2 meters per second has the potential to decrease effective temperature by nearly 2 degrees Celsius by serving as a natural source of ventilation for the body (Budd, 2008).

Additionally, incorporating the impact of solar radiation is another merit of WBGT, because direct sunlight and high solar elevation angle is a driver of environmental heat stress (Otani et al., 2017). Traditional WBGT apparatus uses a black globe thermometer, consisting of a 6-inch black colored sphere fixed with a thermometer inside. When exposed to the outdoor environment, it measures the effects of solar radiation as well as wind speed and temperature. The low albedo black surface of the sphere is an effective absorber of radiation, and thus accounts for the effects of sunlight. In situations characterized by higher sun exposure, the black globe will absorb radiation and heat up more effectively, thus resulting in a higher black globe temperature. Lastly, WBGT considers dry bulb temperature, otherwise known as ambient air temperature, a necessary component of sensing the thermal heat load from the surrounding environment (Budd, 2008).

While WBGT is one of the most comprehensive tools for monitoring hazardous meteorological conditions and guiding appropriate outdoor activity levels, some weighty drawbacks exist. First, the equipment isn't economically feasible for most workplaces and organizations to obtain for on-site use. The top-of-the-line conventional WBGT instrument, such as a QUESTemp°34, that directly measures black globe, dry bulb, and wet bulb temperatures with appropriate thermometers runs just under $3,000 (Cooper et

al., 2017). Even heat stress monitors that closely estimate WBGT components using modeled equations and non-standard black globe thermometers, such as the Kestrel 4400 Heat Stress Tracker, can cost upwards of $600 (Cooper et al., 2017). Traditional WBGT devices are also troublesome to operate. The traditional meter takes roughly 20 minutes for the black globe to calibrate to the surrounding environmental and produce accurate measurements (Lemke & Kjellstrom, 2012), and thus cannot operate instantaneously or continuously. Also, the conventional meters fixed with wet bulb thermometers must be replenished with water to ensure proper reading (Patel et al., 2013). In addition to cost and time-consuming operation requirements, some of the meteorological variables needed to calculate WBGT are not routinely collected. Because of such obstacles, a variety of techniques for estimating and modeling WBGT and its components have been developed to serve as reasonable substitutes. In addition to making monitoring more accessible, such mathematical models using ordinary meteorological data can be used for forecasting capabilities as well as retrospective climate analysis (Patel et al., 2013).

2.4 WBGT ESTIMATION METHODS

Despite its acceptance as the best measure of physiological heat stress, cost and maintenance requirements restrict widespread adoption of WBGT, thus motivating a variety of approximation methods. The intent of such mathematical modeling is to use more accessible meteorological variables to approximate WBGT and to make it accessible to a wider breadth of industries and organizations.

Liljegren Model. One such mathematical model developed to estimate WBGT is the Liljegren model (2008). Highly vetted and cited, it contains equations for both natural wet bulb temperature and black globe temperatures to calculate WBGT measurements.

The meteorological inputs required to run the model includes dry bulb temperature, relative humidity, wind speed, and solar radiation. The tool was motivated out of a need for more accessible WBGT monitoring for workers at chemical storage depots across the U.S. who often wear personal protective clothing that inhibits evaporative cooling. This method incorporates both direct and diffuse solar radiation, and is universally applicable to a range of locations, for it was "developed from fundamental heat and mass transfer principles", meaning that "the models are independent of location and require no local adjustments" (Liljegren et al., p. 654, 2008). The model has proven highly accurate, with its estimates within 1° C of true WBGT measurements. The Liljegren model has been validated and recommended by other researchers for outdoor WBGT measurements (Lemke & Kjellstrom, 2012), and has been used to develop a WBGT climatology to determine regional safety thresholds for athletes across the contiguous United States (A. Grundstein et al., 2015). In an evaluation comparing the Liljegren model to a WBGT estimation model developed by (Matthew et al., 2001), the Liljegren method was determined the most successful and closely aligned with the actual WBGT measurements (Patel et al., 2013) and predicted flag conditions more accurately across the full range of temperatures.

Stull Model. Aside from the Liljegren model to estimate WBGT components, Stull (2011) constructed another mathematical model for estimating the natural wet bulb temperature component of WBGT, using only relative humidity and ambient air temperature as data inputs. The equation is an inverse function for wet bulb temperatures derived through regression methods, in which the model of best fit was selected using wet bulb, ambient temperature, and relative humidity as the input data. It should be noted

that the Stull regression equation contains several assumptions. First, the model is only accurate for conditions at sea level pressure (roughly 1000 millibars), and therefore is not interchangeable across a diverse set of locations. Additionally, the equation is viable only for situations in which relative humidity ranges 5% to 99%, and temperature ranges between -20° C and 50° C. However, if these three assumptions are met, the equation is quite accurate and is simpler to use than the Liljegren model. R^2 values suggests that the regression model predicts 99.95% of wet-bulb temperature values from temperature and relative humidity, with a mean absolute error of 0.28 °C (Stull, 2011).

Black Globe Regression Method. Also, Hajizadeh et al. (2017) used regression modeling to construct an equation for the black globe component based on other standard meteorological variables, which can then be used as an input to calculate WBGT. This evaluation was motivated by lack of recorded measurements of black globe temperatures at weather stations. Natural wet bulb temperature, dry bulb or ambient temperature, relative humidity, and solar radiation were inputted as independent variables to model black globe temperature as the dependent variable. The model of best fit produced an equation for black globe based on solar radiation, ambient temperature, and relative humidity. Site specific meteorological parameters can be used following similar methods presented by (Hajizadeh et al., 2017), to produce best fit models for black globe temperatures.

Black Globe Linear Equation. In addition to constructing regression equations for estimating black globe Dimiceli et al. (2011) offer an alternative method involving a linear equation to solve for black globe temperatures using standard meteorological data. Based on the fourth-degree polynomial for black globe temperature, the authors provide a

set of instructions and equations for calculating this parameter. The required data inputs include ambient temperature, wind speed, atmospheric vapor pressure, barometric pressure, dew point temperature, as well as solar irradiance, and direct and diffuse solar radiation. According to the authors, this estimation method predicted black globe temperatures with an accuracy of 0.5 °F. Although effective, this method requires inputs of less accessible meteorological variables, such as direct and diffuse solar radiation, that make calculating black globe using the provided linear equation less feasible.

Wet Bulb Globe Temperature (WBGT) from Temperature and Relative Humidity

Relative Humidity (%) \ Temperature (°C)	20	21	22	23	24	25	26	27	28	29	30	31	32	33	34	35	36	37	38	39	40	41	42	43	44	45	46	47	48	49	50
0	15	16	16	17	18	18	19	19	20	20	21	22	22	23	23	24	24	25	25	26	27	27	28	28	29	29	30	31	31	32	32
5	16	16	17	18	18	19	19	20	21	21	22	22	23	24	24	25	26	26	27	27	28	29	29	30	31	31	32	33	33	34	35
10	16	17	17	18	19	19	20	21	21	22	23	23	24	25	25	26	27	27	28	29	30	30	31	32	32	33	34	35	36	36	37
15	17	17	18	19	19	20	21	21	22	23	23	24	25	26	26	27	28	29	29	30	31	32	33	33	34	35	36	37	38	39	
20	17	18	18	19	20	21	21	22	23	24	24	25	26	27	27	28	29	30	31	32	32	33	34	35	36	37	38	39			
25	18	18	19	20	20	21	22	23	24	24	25	26	27	28	28	29	30	31	32	33	34	35	36	37	38	39					
30	18	19	20	20	21	22	23	23	24	25	26	27	28	29	29	30	31	32	33	34	35	36	37	39							
35	18	19	20	21	22	22	23	24	25	26	27	28	29	30	31	32	33	34	35	36	37	38	39								
40	19	20	21	21	22	23	24	25	26	27	28	29	30	31	32	33	34	35	36	37	38	39									
45	19	20	21	22	23	24	25	26	27	27	28	29	30	32	33	34	35	36	37	38											
50	20	21	22	23	23	24	25	26	27	28	29	30	31	33	34	35	36	37	39												
55	20	21	22	23	24	25	26	27	28	29	30	31	32	34	35	36	37	38													
60	21	22	23	24	25	26	27	28	29	30	31	32	33	35	36	37	38														
65	21	22	23	24	25	26	27	28	29	31	32	33	34	36	37	38															
70	22	23	24	25	26	27	28	29	30	31	33	34	35	36	38	39															
75	22	23	24	25	26	27	29	30	31	32	33	35	36	37	39																
80	23	24	25	26	27	28	29	30	32	33	34	36	37	38																	
85	23	24	25	26	28	29	30	31	32	34	35	37	38	39																	
90	24	25	26	27	28	29	31	32	33	35	36	37	39																		
95	24	25	26	27	29	30	31	33	34	35	37	38																			
100	24	26	27	28	29	31	32	33	35	36	38	39																			

WBGT > 40

Note: This table is compiled from an approximate formula which only depends on temperature and humidity. The formula is valid for full sunshine and a light wind

Figure 2.1 WBGT Estimation Table, by ABM

Australian Bureau of Meteorology Approximation. Reflecting on the complex mathematical models for estimating WBGT and its components, the Australian Bureau of Meteorology (ABM) provides another estimation method for WBGT. The ABM estimation method is arguably the simplest and most accessible; it only requires ambient temperature and relative humidity and conservatively assumes full sunlight exposure and light wind speeds to approximate WBGT (ABM, 2010). A table can be used to discern

the approximated WBGT using temperature and humidity (Figure 1.2). As previously noted, the effects of solar radiation and wind speed are critical components of human heat stress that make WBGT a preferred metric. As such, the ABM method has been criticized for its assumptions about solar radiation and wind speed. The ABM acknowledges these limitations, stating that the formula could lead to overestimations of heat stress particularly during windy or cloudy conditions when incoming solar radiation is choppier. Such overestimations could initiate “false alarms” in which work is unnecessarily curtailed and contribute to lost work hours.

Considering the potential for lost labor hours associated with a changing climate, improper monitoring could lead to overestimation of heat exposure and unnecessary modification of work, thus jeopardizing more work hours and economic opportunity cost. Together these results suggest that the ABM may be suitable for use during mid-day hours when solar radiation peaks but may be less suitable for morning and evening use when moderate radiation assumptions cannot be met.

CHAPTER 3

METHODOLOGY

3.1 STUDY AREA

Columbia, South Carolina, a southeastern US city, makes up the study area for this analysis. The hot and humid conditions experienced in Columbia, combined with its size and structure makes it an appropriate study area for monitoring heat stress and exposure. The nature of Columbia provides an interesting study area due to its distance from the ocean (approximately 187 km), and the porous nature of soils across central South Carolina which contributes to high maximum temperatures in the summer. Additionally, Columbia does not reap the benefits from a sea breeze compared to cities near the coast.

3.2 DATA COLLECTION

To evaluate WBGT conditions in Columbia and compare the various estimation techniques to true WBGT measurements, WBGT readings were recorded using Kestrel 5400 Heat Stress Trackers. Measurements derived from the Kestrel 5400 will be considered the ground truth observation for the intents and purposes of this study. The selected device provides several benefits compared to other instrumentation options. First, the Kestrel 5400 device measures in-situ meteorological data to calculate WBGT parameters, versus using a mathematical model to construct WBGT, such as the Liljegren model used in prior research (Grundstein & Cooper, 2018). Additionally, the Kestrel 5400 allows for the collection of long and continuous sampling periods, versus a traditional WBGT meter which must be replenished with water and monitored routinely

to produce accurate measurements. It should be noted that the Kestrel 5400 utilizes a smaller than standard black globe (1-inch diameter), versus the traditional 6-inch black globe. As such, the black globe temperatures are estimated through scaling and consider the effects of temperature, wind speed, and solar radiation when exposed to surrounding air. In addition to producing a black globe measurement, the Kestrel 5400 measures dry bulb temperature, and computes natural wet bulb temperature to produce WBGT readings. The prior model (Kestrel 4400) has produced conservative yet accurate gauges for WBGT in trials (Cooper et al., 2017). Finally, this device has been used as the ground truth measurement in prior research evaluating WBGT estimation methods (Carter et al., 2020). At the WBGT measurement site, the Kestrels were mounted on a tripod with a wind vane at a height of 1.5 meters to capture heat exposure conditions at the height of humans.

Two Kestrel 5400 Heat Stress Trackers were deployed at a Cooperative Observer Program (COOP) Weather Station located at the University of South Carolina, Columbia during the first week of July, 2021. One Kestrel was situated on a grass field directly adjacent to the COOP weather station recording site, and the second Kestrel was situated on a brick surface in the same environment, roughly 100 meters away from the Kestrel on grass. This siting scheme was designed to compare heat exposure data on two distinct land surfaces in close proximity, with the goal and assumption that all other factors are held relatively equal. Data collection at the COOP site began on July 8 and continued through the end of September, with several short data gaps due to the Kestrel's data storage limitations and battery life.

Several additional meteorological variables were recorded at the COOP station using Onset HOBO Data Loggers and Kestrel Devices. Literature suggests that microclimate environments may produce thermal heterogeneity throughout a city (Smargiassi et al., 2009) due to a variety of factors such as land surface type, street orientation, and vegetation cover. Thus, several meteorological variables were recorded at the grassy WBGT site immediately next to the Kestrel 5400 to be used as local data inputs for the WBGT estimation methods. Comparing how the estimation methods perform using data inputs at the COOP weather station versus airport weather station data (approximately 2 miles away) will assess if more localized data recorded in the same environment as WBGT measurements improves these estimation methods.

Accordingly, a pyranometer measuring solar radiation in one-minute intervals began recording on July 8th. A Kestrel DROP Fire Weather Monitor was set up in a cotton-region shelter on July 20th. Kestrel DROP monitors are small portable devices that record ambient temperature, dew point temperature, relative humidity, barometric pressure, and psychometric wet bulb temperature. In an analyses comparing the Kestrel DROP monitors to other similar temperature recording devices on the market, the Kestrel DROP was proven to be more accurately aligned with weather station data compared to Thermochron and Hygrochron iButtons (Bailey et al., 2020). Accordingly, the localized temperature and relative humidity data from the Kestrel DROP monitor situated at the COOP station was used as inputs for the selected WBGT estimation methods. Ambient temperature is also necessary for estimating black globe temperature using the linear regression method. On August 12th, a secondary HOBO Onset temperature and relative humidity sensor was deployed, recording one-minute intervals at 1.5 meters. An

anemometer on the same date was mounted to measure wind speed at 2 meters. The HOBO temperature relative humidity sensor serves as another data input for calculating the ABM and Stull estimation methods, and linear regression for black globe temperature. Wind speed from the anemometer provides another data source for modeling black globe temperature.

Hourly weather station data from the nearest Automated Surface Weather Observing System (ASOS) station at Jim Hamilton Owens Airport (KCUB) was used for several WBGT estimation methods. Ambient temperature, relative humidity, and wind speed are required data inputs for ABM estimations, the Stull method, and Hajizadeh method to estimate black globe temperature.

3.3 DATA PROCESSING

Since all variables at the COOP site were recorded in 1-minute intervals and the KCUB weather station reports data once hourly, all COOP data were aggregated to an hourly value in a manner consistent with the National Weather Service (NWS) reporting scheme. In accordance with ASOS reporting, ten 1-minute data values from the COOP station immediately before the published time were averaged together, to represent an hourly average for each variable. For example, KCUB hourly data values are reported by the NWS 53 minutes after the top of every hour. Accordingly, the ten 1-minute recordings between 40 and 50 minutes of each hour were averaged together to represent an hourly value. This aggregation scheme was used for temperature, relative humidity, wind speed, and solar radiation across all COOP 1-minute data for WBGT estimations.

3.4 ESTIMATING WBGT USING ABM METHOD

The first goal of this analysis is to evaluate how well WBGT can be estimated using various methods and data sources, in lieu of traditional WBGT instrumentation. Three estimation methods were used including 1) the ABM method to compute WBGT using temperature and relative humidity, as well as 2) the Stull equation to estimate wet bulb temperature using temperature and relative humidity and 3) the Hajizadeh for estimating black globe temperatures. The ABM estimation method provides the full WBGT metric, the wet bulb and black globe estimates from Stull and Hajizadeh, respectively, were combined to compute the full WBGT metric using Equation [1].

These estimation methods were calculated using meteorological data from two sources: the nearest ASOS weather station, and localized portable weather monitors in close proximity to the Kestrel 5400 WBGT recording sites. For the Columbia analysis, this includes the solar radiation, ambient temperature, relative humidity, and wind speed from the COOP weather station.

First, the ABM method was used to estimate WBGT using a simple equation [2] (American College of Sports Medicine, 1984), where variable *p* represents water vapor pressure, which is calculated from relative humidity and air temperature using Equation [3]. Accordingly, the ABM estimated WBGT will be compared against measurements from the Kestrel 5400 device. To account for local temperature variability, WBGT was calculated using ABM equation twice, once using temperature and relative humidity data from the nearest airport weather station (KCUB) and a second time using localized data from the in-situ weather monitors which includes the COOP Kestrel DROP.

$$\boldsymbol{WBGT = (0.567 \times T_{db}) + (0.393 \times p) + 3.94} \quad \textbf{[2]}$$

$$\boldsymbol{p(hPa) = \left(\frac{RH}{100}\right) \times 6.105 e^{\frac{(17.27 \times T_a)}{(237.7 + T_a)}}} \quad \textbf{[3]}$$

3.5 ESTIMATING WET BULB AND BLACK GLOBE TEMPERATURE

Wet bulb temperatures were estimated using the Stull (2011) equation [4]. Columbia, South Carolina is situated at the appropriate sea level pressure, and we do not anticipate outdoor temperatures deviating from -20° C and 50° C. Accordingly, the Stull equation is appropriate to use in this study area. The Stull method requires only ambient air temperature and relative humidity to derive wet bulb temperature estimates.

Like the ABM estimates, WBGT was calculated twice to account for local temperature variability. The first time uses temperature and relative humidity data from the nearest airport weather station (KCUB) and a second time uses localized data from the portable weather monitors situated in the WBGT measurement area.

$$\boldsymbol{T_{wb} = T_a \times arctan[0.151977 \times (RH\% + 8.313659)^{\left(\frac{1}{2}\right)}] + arctan(T_a + RH\%) - arctan(RH\% - 1.676331) + 0.00391838 \times (RH\%)^{\left(\frac{3}{2}\right)} \times arctan(0.023101 \times RH\%) - 4.686036} \quad \textbf{[4]}$$

Since the Stull equation only produces the wet bulb temperature component of WBGT, it is necessary to compute black globe temperature by some other means. Figure 3.1 visualizes the estimation methods that will be used to calculate each WBGT subcomponent. Accordingly, black globe temperature was estimated using a linear regression method, similar to that of Hajizadeh et al. (2017) who used wet bulb temperature, ambient temperature, solar radiation, and relative humidity as the independent variables, to model observed black globe temperature. Their final linear equation modeled black globe temperature using solar radiation, ambient temperature,

and relative humidity. For this study, a similar methodology was followed to model the known black globe temperature measured by the Kestrel 5400 over grass. However, ambient temperature, relative humidity, solar radiation, and wind speed were selected as the potential input variables to fit the regression equation based on data availability.

Black globe temperature, as noted previously, was computed twice, once using ASOS weather station data from KCUB and a second time using localized data sources in at the COOP site. The KCUB estimated black globe temperature will include ambient temperature, relative humidity, wind speed data from KCUB, and solar radiation collected at the COOP site (since solar radiation data is not available at KCUB). 10-meter wind speed obtained from the airport weather station was downscaled to 2-meter wind speeds, to be consistent with Kestrel 5400 measurement height and COOP wind speed height. This was accomplished using an equation for grass surfaces provided by Allen et al., 1998. The second black globe temperature regression model was run entirely using local data sources collected at the COOP weather station site immediately next to the Kestrel 5400 Heat Stress Tracker (including ambient air temperature, relative humidity, solar radiation, and 2-meter wind speed). All of the selected WBGT estimation methods, their components, and equations are summarized in Figure 3.1.

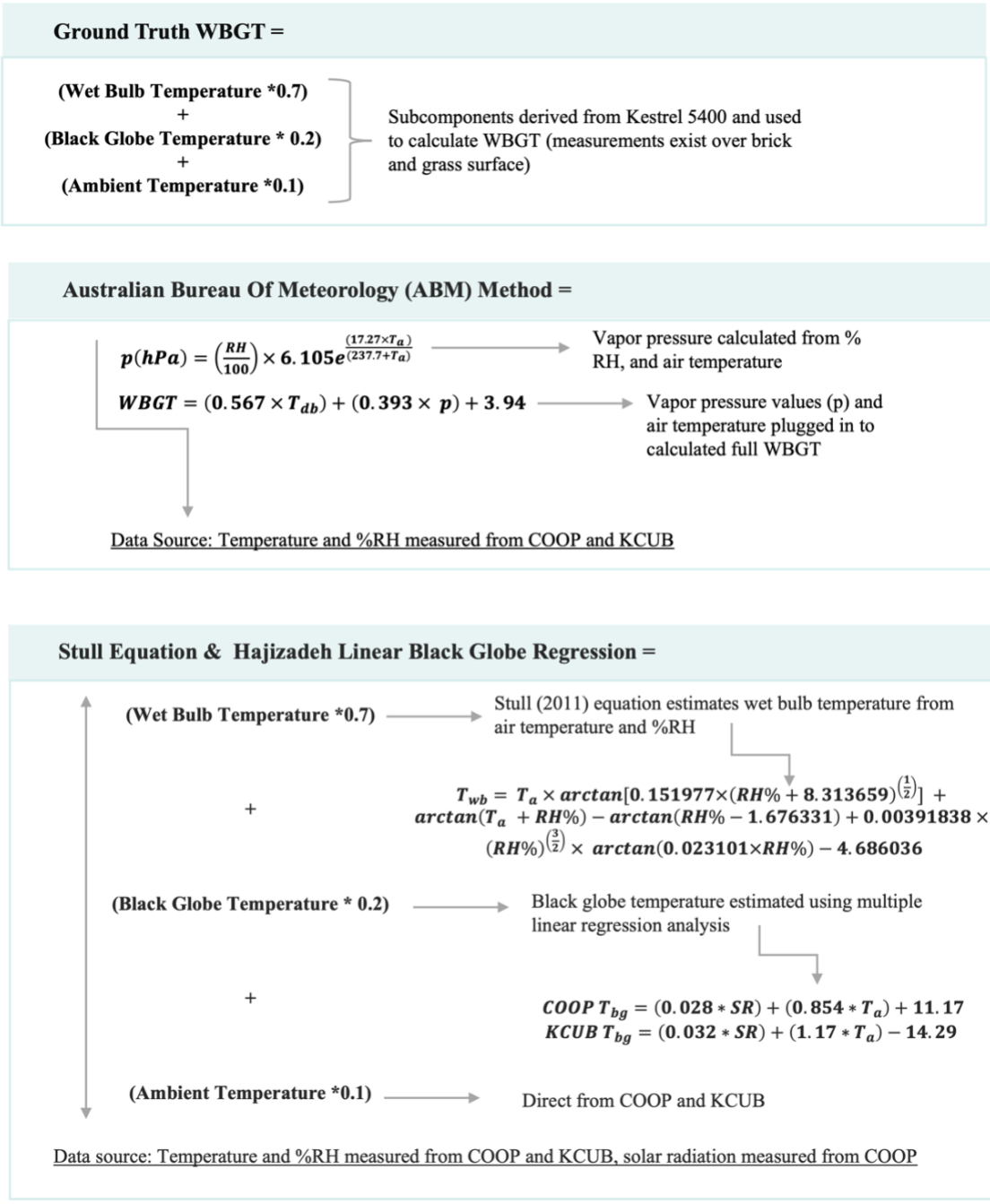

Figure 3.1 Summary of WBGT Estimation Method Scheme

3.6 STATISTICAL ANALYSIS

A variety of statistical methods evaluate how closely these models predict WBGT. The WBGT recordings over both grass and brick surfaces are evaluated against the Kestrel ground truth measurements, with the grass measurements used for various subsets

of data. A suite of difference measures will be used to assess model performance, versus correlation coefficients and r^2 values. This is because the latter do not assess observed versus estimated variables between models, but rather describes the strength of their relationship (Willmott, 1982). Alternatively, root mean square error (RMSE) and mean absolute error (MAE) are appropriate indicators of model performance, as they describe the degree to which observed versus modeled values deviate. Accordingly, model fitness will be evaluated based on MAE, RMSE, and the index of agreement (d). Willmott's d index describes model performance error and can be used to cross compare the different WBGT estimation methods. A *d* value close to 1 suggests complete model performance, and values approaching zero suggests lack of agreement. In other words, higher d values approaching 1 suggest more optimal model performance. Finally, Mean Bias Error (MBE) will be used to assess directionality of relationships and determine if the models tend to over or underestimate WBGT.

Literature suggests that WBGT values may vary in performance at different times of day and under different weather conditions (Carter et al., 2018, Grundstein & Cooper, 2018) . Accordingly, the ground truth measurements and estimated WBGT values for all models on the grass surface were subset into several categories. Estimated and observed WBGT values at different daily time periods were partitioned for analysis, to produce morning (7:70 AM- 10:50), midday (11:50 – 13:50), and afternoon (14:50 PM – 17:50) measurement subsets. Additionally, estimated and observed WBGT measured during various weather conditions were subset according to weather observations designated by the NWS 3-Day History at KCUB airport. WBGT measurements that coincide with hours marked as "fair" and "a few clouds" were separated to evaluate model performance in

relatively clear and fair-weather conditions. Hours with weather characterized by “partly cloudy”, “mostly cloudy”, “overcast”, “fog”, and any “rain” and “thunderstorm” conditions were separated to evaluate model performance during cloudy and rainy weather. These subsets were calculated only for measurements on the grass surface, for the full data record. MAE, RMSE, MBE, and d indexes were calculated for all measurement subsets.

A robust sampling scheme was designed to ensure independence of observations, and avoid issues associated with autocorrelation. Since many pairs of the estimated and observed WBGT occur over consecutive hours, it was necessary to sample in a manner that ensured data pairs were truly random. For example, calculating difference measures for back to back WBGT observations would violate assumptions of independence, because these data are likely correlated due to their closeness in time. To address this, 40 pairs of estimated and observed WBGT were randomly selected to calculate the four difference measures, and this process was repeated 1,000 times. For data subset at different times of day, 30 WBGT pairs were randomly sampled to calculate difference measures, and 35 random pairs were sampled for the weather subset observations. This scheme addresses autocorrelation due to its repeated random sampling, and also provides 1,000 values for MAE, RMSE, MBE, and d index. These 1,000 values were used to construct violin plots, to visualize deviations between the observed Kestrel WBGT measurements, and the modeled WBGT estimates.

Finally, Analysis of Variance (ANOVA) tests were conducted for the 1,000 MAE values of each model within each subset, to identify if the MAEs of the four models are significantly different from one another. In other words, this can determine if a particular

model performs significantly better, or worse, than the others in each group, or if any difference between models is statistically insignificant. Since observations for the Stull & BGR models were available for one month, and observations for the ABM model were available for a longer three month period, violin plots and MAE values for each of the ABM models during the congruent one month period was compared to the three month record. Mann-Whitney U Tests were performed for the ABM models on both brick and grass, to determine if the one-month and three-month ABM estimates were significantly different. All statistical analysis were executed in R and Microsoft Excel.

After evaluating the ABM and Stull & BGR methods, WBGT was estimated using only wet bulb and dry bulb temperatures using multiple linear regression. The intent of this was to assess if these variables, conveniently measured using a sling psychrometer, can serve as a reasonable proxy method for WBGT. To investigate this, the multiple linear regression analysis was executed using SPSS software with WBGT recorded by the grass Kestrel 5400 from July 20th through August 22nd, as the dependent variable. The independent variables included wet bulb and dry bulb temperatures. To ensure independence from the Kestrel 5400 device, wet bulb temperature was calculated using temperature and relative humidity values from the adjacent Kestrel DROP monitor using the Stull (2011) equation [4]. Dry bulb temperature was measured directly from the Kestrel DROP monitor. For the regression analysis, 50 observations were used to construct a linear equation that predicts WBGT using wet and dry bulb temperatures [5]. This model is characterized by an R^2 value of 0.907, and individual p-values of 0.004 for wet bulb, and 0.00 for dry bulb temperatures, thus indicating that these two predictor

variables are significant. Additionally, VIF statistics of 3.5 for both independent variables indicates that this model is free of collinearity.

$$\boldsymbol{WBGT = (0.654 * T_{wb}) + (0.78 * T_a) - 32.4} \quad \textbf{[5]}$$

The regression equation [5], or the Wet Bulb Regression (WBR) method was used to calculate WBGT on an independent set of data points, in order to assess the model's accuracy. The same sampling scheme used to measure error for the ABM and Stull & BGR models was also used to validate the model depicted by equation [5]. To ensure independence of observations, 40 pairs of observed and predicted WBGT were randomly sampled and used to calculate MAE, RMSE, MBE, and d index. This method was repeated 1,000 times, to evaluate the potential range of error associated with the WBR model. Lastly, the 1,000 values for the four test statistics were used to construct violin plots to assess the accuracy of this novel WBGT estimation method, and compare against the other four models tested in this study.

3.7 LAND SURFACE ANALYSIS

WBGT was recorded using a Kestrel 5400 on a grassy field, and a brick walkway at the COOP weather station in Columbia, SC. Given that two Kestrels were deployed simultaneously within the same environment and geographic vicinity, this study presents a unique opportunity to evaluate how heat exposure may manifest differently across two microclimates. Due to rapid urbanization and land use change that contributes to the urban heat island effect, the deviations in temperature and WBGT values across different land surface characteristics and times of day is a question of considerable interest.

Figure 3.2 Photo of Kestrel on Grass Site at COOP Station

Thus, delta values between WBGT on the brick and grass surfaces, as well as the other atmospheric variables that influence WBGT, were calculated hourly. This analysis only included measurements on the grass and brick surfaces with the same time stamp to compare heat characteristics on the two surfaces with the same conditions. Delta values for several weather variables were calculated for each hour of the day by subtracting grass from brick measurements. All measurements were separated by each hour of the day, creating twenty-four subsets of delta values. To ensure independence, 50 brick and grass measurements recorded at the same exact minute were randomly selected, and the difference was calculated. This was repeated 1,000 times to generate 1,000 difference values between variables on the brick and grass surface, at each hour of the day. Differences for ambient temperature, relative humidity, wind speed, heat index, dew point temperature, and wet bulb temperature were calculated using the Kestrel 5400 device for all 24 hours of the day to express the diurnal change in these variables across both measurement sites. Differences between WBGT and black globe temperature were

calculated only during daytime hours (8:00 to 18:00), because the solar radiation component becomes negligible at night. Violin plots were created to visualize the difference between grass and brick for each variable and its fluctuations throughout the day. Since grass measurements were subtracted from brick, positive delta values indicate higher values on brick, and delta values less than zero indicate higher values on grass. All sampling and analysis were executed using R software. A summary table of all comparisons in the analysis is synthesized in Table 3.1.

Table 3.1 Summary of comparisons for WBGT estimates and land surface analysis

WBGT Estimation Scheme	**Input Variables**	**Data Source**
Kestrel vs. ABM WBGT	Temperature and % RH	COOP
Kestrel vs. ABM WBGT	Temperature and % RH	KCUB
Kestrel vs. Stull Wet Bulb Temperature + Black Globe regression	Temperature and % RH, + Solar, Temperature	COOP
Kestrel vs. Stull Wet Bulb Temperature + Black Globe regression	Temperature and % RH, + Solar, Temperature	KCUB (with COOP solar)
Land Surface Analysis	**Variables**	**Timescale**
Kestrel measurements on Brick vs. Grass	WBGT	8:00-18:00
	Black Globe Temperature	8:00-18:00
	Temperature	24 hours
	Relative Humidity	24 hours
	Heat Index	24 hours
	Wind speed	24 hours
	Dew point Temperature	24 hours
	Wet Bulb Temperature	24 hours

CHAPTER 4

RESULTS

4.1 BLACK GLOBE TEMPERATURE ESTIMATES

Black globe temperature was estimated using linear regression analysis and paired with wet bulb temperature derived from the Stull equation, in order to calculate the full WBGT metric. The multiple linear regression analysis for black globe temperature was performed using SPSS Statistical Software. Data during the hours 8:00 to 18:00 were used for this analysis, because measurements recorded outside of daylight hours are negligible due the impacts of solar on black globe temperature. To perform the preliminary analysis before the linear regression analysis, Kestrel black globe temperature, COOP measured solar radiation, wind speed, temperature, and relative humidity were gathered. However, measurements for all five of these variables were only available over congruent times for a two week period between August 12th through August 26th, with several gaps due to haphazardly missing data. After data were processed and aggregated at an hourly value (as described in section 3.3), 125 and 112 data points for the COOP and KCUB sites, respectively, were used to construct the regression model. Preliminary data analysis was performed to assess correlations and directionality between black globe temperature and each independent variable from both data sources. Scatterplots between the dependent variable, and each predictor variable were produced to determine if relationships between variables were in fact linear.

Additionally, Pearson's correlation coefficients for black globe temperature and each independent variable were produced in Microsoft Excel, to determine the strength of the relationships using R values.

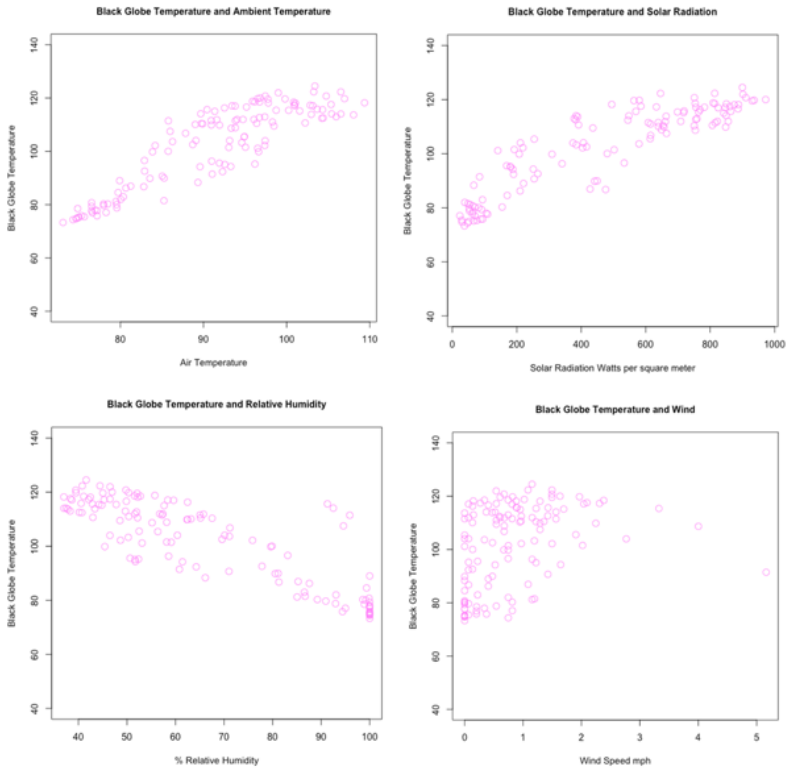

Figure 4.1 Relationships between Black Globe Temperature and COOP measured Independent Variables (Temperature, Solar, Relative Humidity, and Wind)

For the COOP data, strong linear relationships were found between black globe temperature and ambient temperature, solar radiation, and relative humidity (Figure 4.1) with Pearson's R values of 0.88, 0.89, and -0.84, respectively. These strong positive relationships are expected, because as peak temperature and solar radiation increase, black globe temperature should also rise. The negative relationship between black globe temperature and relative humidity is also as expected, because when black globe temperature peaks during the hottest afternoon hours, relative humidity is at its lowest diurnally. Wind speed exhibited weak relationships with black globe temperature, with a

Pearson's R value of 0.34. Previously it was theorized that wind speed would have a negative relationship with black globe temperature, as air ventilation should theoretically serve as a cooling mechanism. Due to the relatively weak and nonlinear relationship of wind speed and black globe temperature, as designated by the scatterplot in Figure 4.1 and low Pearson's R value, wind speed was excluded as an independent variable in the regression analysis.

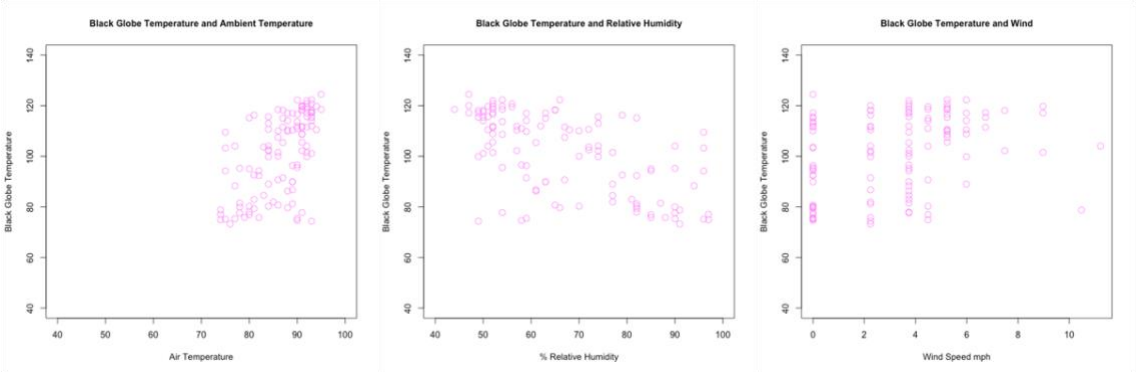

Figure 4.2 Relationships between Black Globe Temperature and KCUB measured Independent Variables (Temperature, Relative Humidity, and Wind)

Similarly, ambient temperature and relative humidity from the KCUB station exhibited strong linear relationships with black globe temperature, with Pearson's R values of 0.89, and -0.85, respectively (Figure 4.2), signifying these variables were suitable for the linear regression analysis. According to Figure 4.2, relationships between wind speed and black globe did not exhibit a linear pattern, and had a Pearson's R of 0.25, suggesting a weak relationship. Thus, wind speed was also excluded as a dependent variable for the regression analysis for KCUB data model.

Four models were produced using linear regression analysis in SPSS software to predict black globe temperature based on different independent variables and data sources. For the COOP data, Model 1 predicted black globe temperature from three independent variables (ambient temperature, solar radiation, and relative humidity).

COOP Model 2 predicted black globe temperature from just two independent variables (ambient temperature, and solar radiation). For Model 1, regression results indicated that relative humidity had a p-value of 0.38, which is greater than alpha value of 0.05, suggesting a lack of significance. Additionally, temperature and relative humidity had variable inflation factors (VIF) greater than 7, suggesting collinearity between these variables. Accordingly, the regression was re-run omitting relative humidity as an independent variable. In the resulting Model 2, both independent variables had significant p-values and VIF statistics of 1.7, suggesting this model was free of correlated variables. COOP Model 1 (3 variables) had an R^2 value of 0.96, and Model 2 (2 variables) had an R^2 value of 0.959. For both equations, the residual plots suggest randomness, thus meeting an essential assumption of linear regression equation (Figure 4.3).

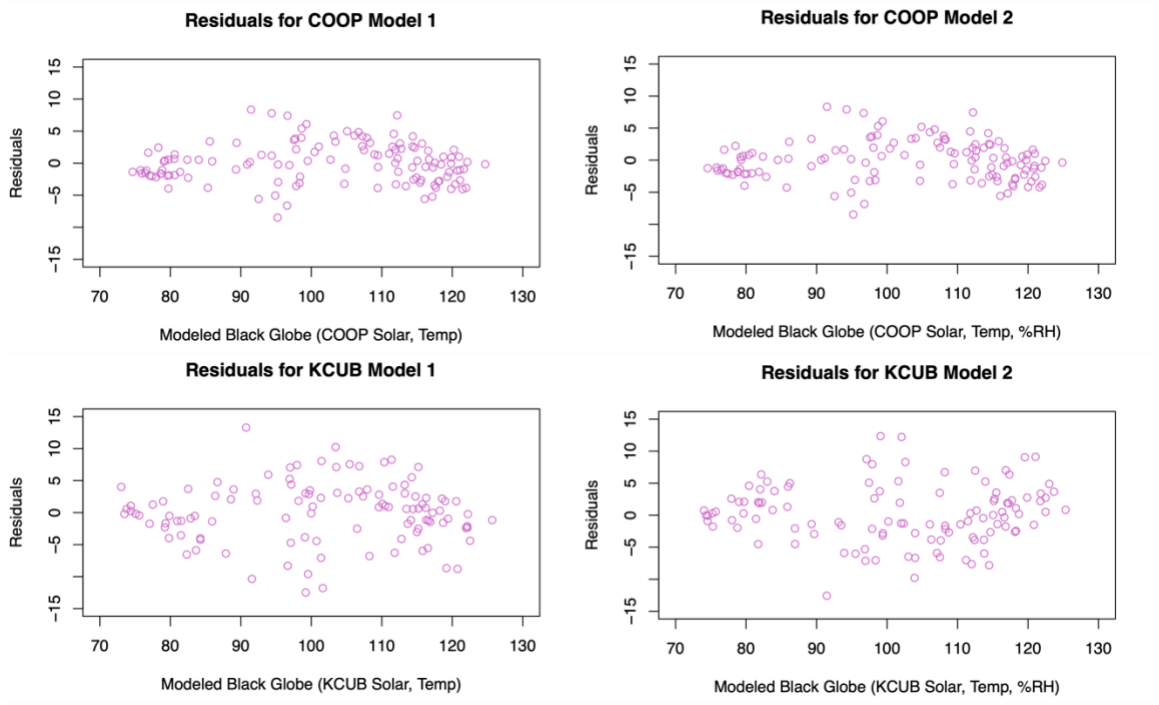

Figure 4.3 Residual Plots for COOP and KCUB Models

The models derived from KCUB data produced similar results. Model 1 (3 variables) from KCUB contained an insignificant independent variable, and temperature

and relative humidity were both characterized by high VIF values suggesting collinearity in the model. The same procedure as the COOP regression was followed; the linear regression was re-run omitting relative humidity as an independent variable. KCUB Model 2 using solar radiation and temperature as independent variables yielded more promising results. Both variables were characterized by p-values below 0.05, and VIF statistics for both variables were both 1.7. In Model 1, R^2 value suggests 91.4% of the variance of black globe temperature is explained by the three independent variables in the model, and 91% of the dependent variable is explained by the two independent variables of Model 2. Additionally, the residual plots for KCUB models indicate that the residuals have a random pattern dispersed around zero (Figure 4.3).

For both the COOP and KCUB weather stations, the models using temperature and solar radiation as independent variables (COOP Model 2 and KCUB Model 2) performed the most optimally. This was determined based on the fact that the two independent variables in these models were statistically significant, and collinearity tests suggest these models are free from correlated variables. Additionally, Figure 4.3 suggests that the residuals from these models show independence and randomness. Accordingly, the final linear equations that were used to model the black globe temperature component of WBGT using in-situ COOP data inputs are as follows:

$$\boldsymbol{COOP\ T_{bg} = (0.028 * SR) + (0.854 * T_a) + 11.17} \quad \textbf{[6]}$$

And KCUB temperature inputs:

$$\boldsymbol{KCUB\ T_{bg} = (0.032 * SR) + (1.17 * T_a) - 14.29} \quad [7]$$

Black globe temperature was then calculated using these equations, and applied to the full data record to calculate WBGT in full.

4.2 ESTIMATION METHOD RESULTS

The selected estimation methods yielded four different ways of modeling WBGT, including COOP and KCUB ABM models, and the Stull & Black Globe Regression (BGR) models for the COOP and KCUB sites. These four modeled estimates were compared against ground truth WBGT recorded by the Kestrel. The violin plots for all groups of models were generated using 1,000 measures of randomly sampled pairs of observed and predicted WBGT to achieve error bars around the performance metrics. Each violin plot displays the distribution of MAE, RMSE, MBE, and d index calculated for each model. The violin plots not only depict the spread of error for each estimate, but also the distribution of data making them informative visualization tools for evaluating model performance. The widest segments of the violin plots suggest the greatest frequency of corresponding values, and thinner parts indicate fewer observations at a particular value.

ANOVA tests determined if MAE values, and therefore model performance, was significantly different across the four models for each data subset. Results from the ANOVA and Tukey post hoc tests indicates that in most cases, MAE values statistically differ for the four models, with some exceptions. MAE values for the Stull COOP and ABM KCUB ($p=0.924$) in fair weather, ABM COOP and ABM KCUB ($p=0.608$) during morning hours, and Stull KCUB and ABM COOP ($p=0.592$) during afternoon hours were statistically indistinguishable.

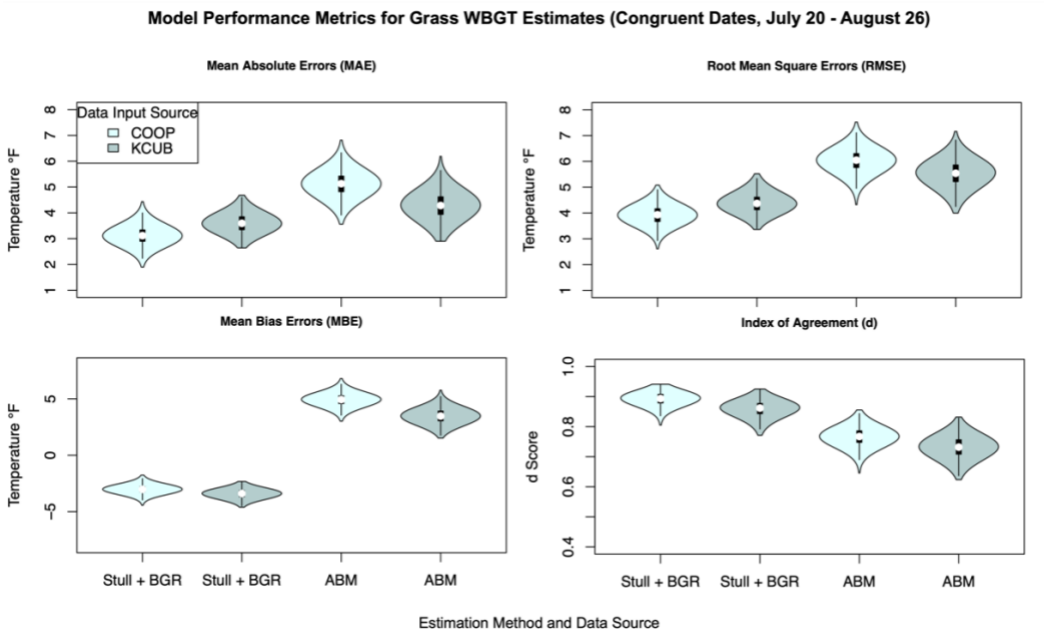

Figure 4.4 Violin Plots for Model Performance Metrics (Grass, Congruent Dates)

WBGT estimation performance during the full record of data. When the four models were calculated over a congruent one-month period, the Stull & BGR models tended to estimate WBGT more accurately compared to the ABM models (Figure 4.4). According to Table 4.2, the Stull & BGR models were characterized by mean MAEs of 3.12° F (COOP data) and 3.6° F (KCUB data), which is markedly lower compared to ABM models with mean MAEs of 5.12° F (COOP data) and 4.28 °F (KCUB data). MBE values suggest that the Stull & BGR models consistently underestimate WBGT while the positive MBE values indicates that the ABM method overestimates WBGT (Figure 4.4). Additionally, the Stull & BGR models had index of agreement (d) values approaching 1, suggesting stronger agreeance between modeled estimates and observed WBGT, compared to the ABM models. The ABM models appear to have a wider range of d values as low as 0.7, further indicating that the ABM models are less favorable than the Stull & BGR estimates. Finally, estimation performance for the Stull & BGR models was

improved when local COOP data were used as inputs, versus the KCUB data, which is made evident by lower MAE and RMSE values. Alternatively, the ABM estimates performed more optimally when KCUB airport data inputs were used, versus the local COOP data.

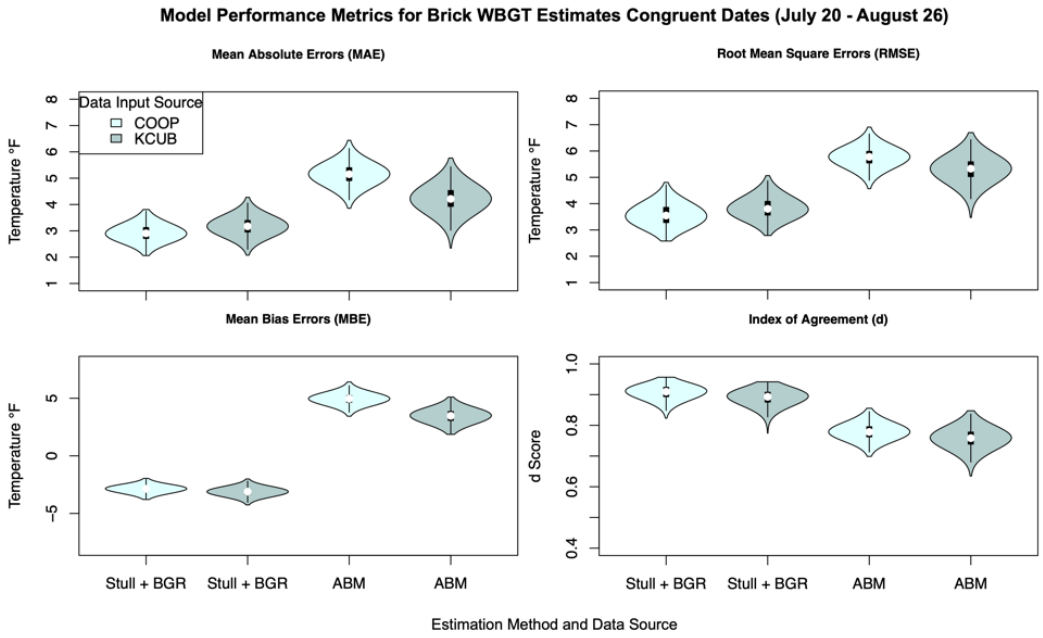

Figure 4.5 Violin Plots for Model Performance Metrics (Brick, Congruent Dates)

The performance of these WBGT estimation methods on the grass surface are rather comparable to performance on the brick surface (Figure 4.5). For the ABM model, MAE values on brick were markedly similar to those on grass, with mean MAE values of 5.15° F (COOP data) and 4.21° F (KCUB data). For the Stull & BGR models, the brick estimates were slightly lower than those on grass, with mean MAE values of 2.91° F (COOP data) and 3.17° F (KCUB data). Consistent with previous results at the grass site, the ABM models overpredicted WBGT while the Stull & BGR models underestimated it, indicated by the MBE values. Like the grass estimates, the two different data input sources impacted the WBGT estimates. Based on MAE and RMSE values (Figure 4.5)

COOP data improved estimated WBGT values for the Stull & BGR model, while KCUB data produced lower errors for the ABM model.

Figures 4.4 and 4.5 display violin plots for model performance measures calculated over a congruent one-month period on the grass and brick surfaces (July 20-August 26). However due to data availability, it was also possible to calculate the ABM models for a longer three-month record (July 20-September 30). Accordingly, performance metrics for the ABM models over the three-month record were calculated and compared against the ABM performance during the one-month record. The ABM performance statistics over the 3-month record appear visually similar to the congruent one-month record, with a few minor exceptions. Across both the brick and grass sites, the Stull & BGR models continue to outperform the ABM model, which is made evident through lower MAE and RMSE values (Table 4.2). Parallel with previous results, the localized COOP data improves accuracy of the Stull & BGR models, while the ABM model performs more optimally when KCUB data are used. Also, the directionality of the two estimates is the same as in previous results, where negative MBE values suggest underprediction of the Stull & BGR methods, and positive MBE values indicates overprediction of ABM models. The main difference between the one and three month data record is the index of agreement values. On both the brick and grass surface, the ABM models are characterized by a much larger range in d values over the longer data record. With the addition of the two months of observations, the d values range from roughly 0.9 to as low as 0.6 on the grass surface, and 0.65 on bricks. Alternatively, d index values are limited from roughly 0.8 to 0.6 over the congruent dates, suggesting that ABM calculated over the longer record led to slightly more erratic ranges in d index.

Table 4.1 Descriptive statistics for MAE values

Data Subset	MAE Statistics	Stull BGR (COOP)	Stull BGR (KCUB)	ABM (COOP)	ABM (KCUB)
Grass (full record)	*Mean*	3.12	3.6	4.58	4.33
	Max.	4.43	4.68	5.99	6.06
	Min.	1.89	2.64	3.26	2.62
Brick (full record)	*Mean*	2.91	3.17	4.57	4.2
	Max.	3.81	4.27	5.95	5.99
	Min.	2.06	2.07	3.15	2.60
Grass (congruent dates)	*Mean*			5.12	4.28
	Max.			6.81	6.19
	Min.			3.56	2.90
Brick (congruent dates)	*Mean*			5.15	4.21
	Max.			6.43	5.76
	Min.			3.85	2.34
Fair Weather	*Mean*	3.61	4.07	3.91	3.602
	Max.	4.64	5.32	5.28	5.16
	Min.	2.51	2.93	2.66	2.01
Cloudy Weather	*Mean*	2.17	2.93	6.21	5.44
	Max.	3.03	3.95	7.52	6.71
	Min.	1.23	1.91	4.92	3.61
Morning	*Mean*	1.86	2.22	6.25	6.23
7:50-10:50	*Max.*	2.79	3.05	7.34	7.86
	Min.	1.11	1.21	4.97	4.61
Midday	*Mean*	4.04	4.39	3.27	3.07
11:50-13:50	*Max.*	4.86	5.26	4.54	4.25
	Min.	3.36	3.62	2.15	2.07
Afternoon	*Mean*	3.37	4.11	4.13	3.52
14:50-17:50	*Max.*	4.24	5.15	5.55	4.75
	Min.	2.54	3.11	2.81	2.01

Results from Mann-Whitney U Test suggests that the ABM method's magnitude of errors differ significantly as a function of measurement period. Except for the estimation of WBGT on the brick surface using KCUB data, MAE values differed significantly when calculated for a one-month versus a three-month period. This suggests potential temporal inconsistencies in the ABM estimation method.

Table 4.2 Mann-Whitney U Test Results for MAEs from ABM Models over a 1 month versus 3 month record

Data Subset	Model	p-value
Grass, 1 month vs. 3 month record	ABM COOP	2.2e-16
	ABM KCUB	0.033
Brick, 1 month vs. 3 month record	ABM COOP	2.2e-16
	ABM KCUB	0.561

Impact of Data Source on estimations. The same trends in WBGT model performance and behavior that appeared over the full scope of observations, also present themselves when data are subset under different weather conditions and times of day, with some exceptions. First, only half of the models performed better using localized data than airport data. The Stull & BGR models had lower mean MAE values when using local COOP as opposed to KCUB data, for all weather condition and time of day subsets. However, the use of COOP data for the ABM models lead to larger overestimates of WBGT, as mean MAE values were consistently higher when localized COOP data were used versus KCUB data. Ultimately, this suggests a consistent pattern of the Stull & BGR models being improved when in-situ data are used, but ABM performing more favorably with airport data.

Error Directionality. Second, the directionality of model error was uniform across data subsets. Across the entire data record, the Stull & BGR models underestimate

WBGT, while the ABM models consistently overestimate it. This tendency exists during sunny weather conditions (Figure 4.8), periods of cloud and rain cover (Figure 4.6), as well as during isolated morning (Figure 4.7), midday (Figure 4.9) and afternoon hours (4.10). Notably, MBE values steadily mirror MAE values across all scenarios, suggesting that the directionality of estimation error is rather consistent across all models. Alternatively, if MBE values were closer to zero, this would indicate that the models were over and underpredicting WBGT at similar frequencies, indicating a more erratic nature to the estimation error. However, the somewhat identical magnitudes of MBE and MAE across models indicates a rather consistent tendency for Stull & BGR model to underestimate, and for ABM to overestimate values.

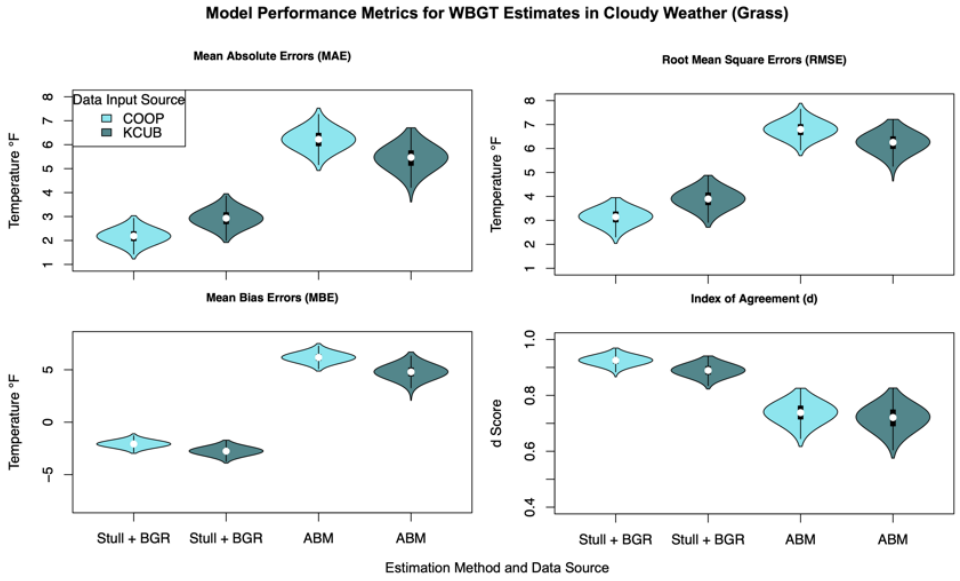

Figure 4.6 Violin Plots for Model Performance Metrics (Grass, Cloudy and Rainy Weather)

Magnitude of model error under different scenarios. Third, while the directionality of model error is uniform across different conditions, there are certain scenarios where the magnitude of error changes dramatically across the models. Notably,

these estimation methods perform at varying levels of efficacy during different weather conditions and times of day. The tendency for ABM to overestimate WBGT values is inflated during periods of cloud and rain (Figure 4.6), and during morning hours (Figure 4.7). Model estimates subdivided under cloudy and rainy weather conditions demonstrate that the ABM models overestimate WBGT significantly, with mean MAEs of 6.2 °F (COOP) and 5.4 °F (KCUB). At best, the ABM models overestimated WBGT by 4.92° F (COOP data) and 3.61° F (KCUB data) under these weather conditions, as indicated by minimum MAE values (Table 4.1). Alternatively, the Stull & BGR models are more accurate, with mean MAEs of 2.1 °F (COOP data) and 2.9 °F (KCUB data).

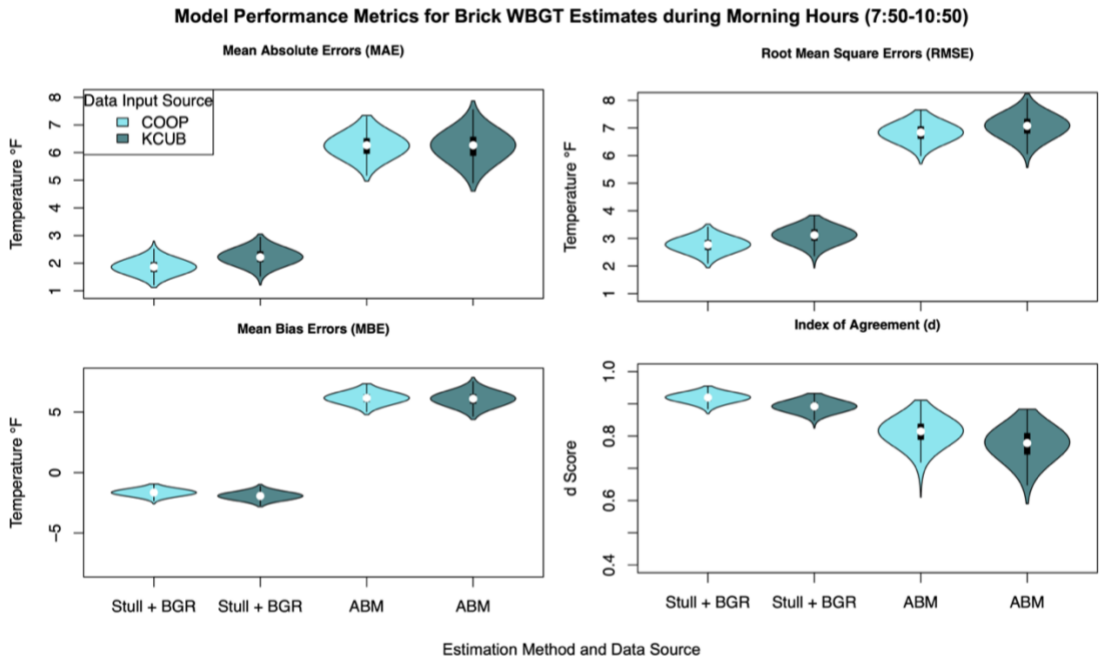

Figure 4.7 Violin Plots for Model Performance Metrics (Grass, Morning Hours)

Modeled WBGT during the morning hours of 7:50 to 10:50 displays similar relationships to those in cloudy conditions. Both Stull & BGR models performed significantly better than ABM estimates, with mean MAE values of 1.8 °F (COOP data) and 2.2 ° F (KCUB data). On the other hand, ABM drastically overestimated WBGT

during early morning hours, with mean MAEs of 6.3 °F (COOP data) and 6.2° F (KCUB data). While there was no statistical difference in MAEs between the two ABM estimates with different data sources, both the Stull & BGR models performed significantly better than both ABM models from 7:50 to 10:50.

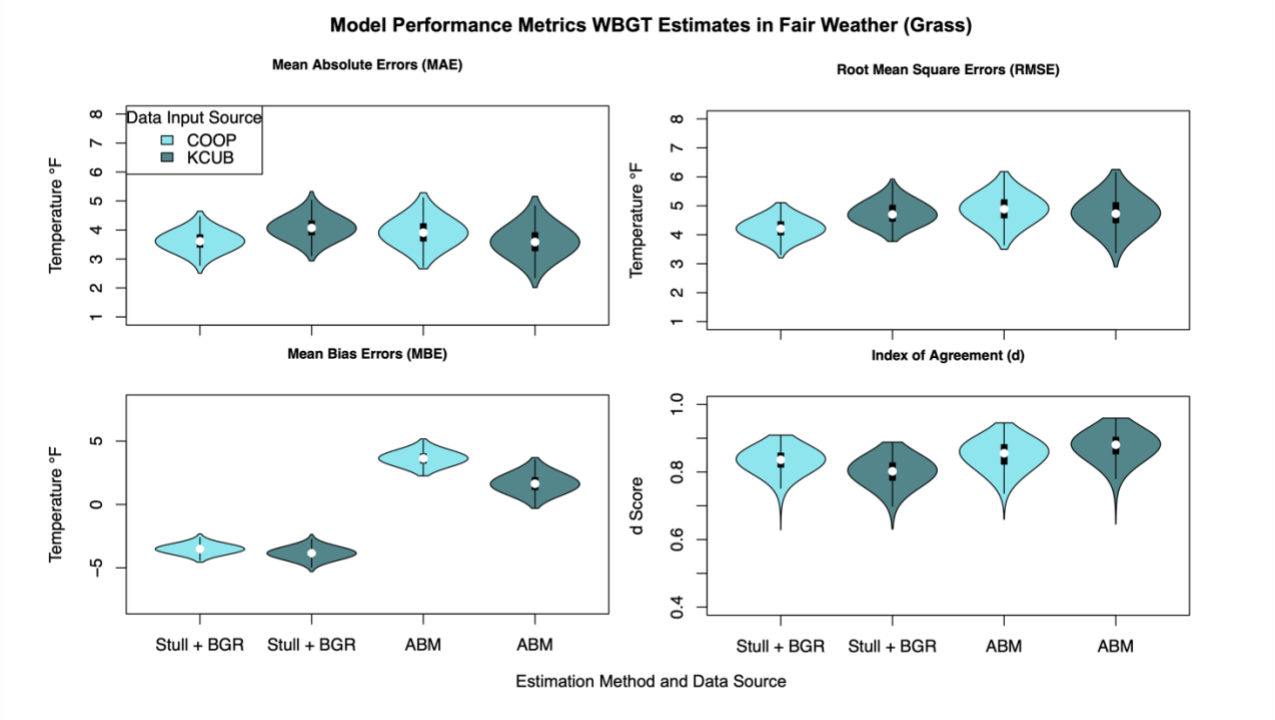

Figure 4.8 Violin Plots for Model Performance Metrics (Grass, Fair Weather)

Despite the tendency for ABM to overpredict WBGT in certain cases, there were some occasions in which it performed in a manner comparable to Stull & BGR models. During fair weather conditions, model performance improved for ABM estimates in comparison to estimates made during the whole data record (Figure 4.9). MAEs for all four models under fair weather conditions were somewhat comparable, with means of 3.6 °F, 4.1 °F, 3.9 °F, and 3.6 °F. In this subset, MAE values for the four models were significantly different from one another, except for the Stull & BGR (COOP data) and

ABM (KCUB data), as shown by the post hoc Tukey adjusted p-value of 0.92 in Table 4.3. Since these two models are the best performing in this subset, the nonsignificant difference between their MAE values suggests these methods perform similarly in fair weather. Additionally, the lengthier violin plots suggest that MAE, RMSE, and d index values have a greater error range compared to the full data record. In particular, d index values across the four models range from 0.9 to 0.6. This suggests that while error for ABM estimates is improved during fair weather conditions, both models tend to estimate WBGT across a larger spread of values, rather than being consistently estimated within a confined range.

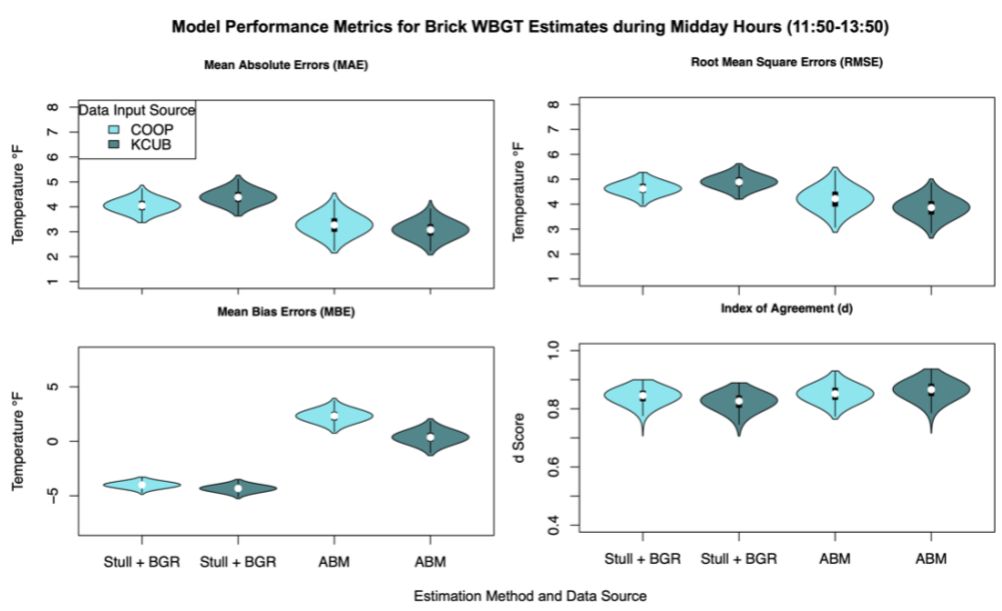

Figure 4.9 Violin Plots for Model Performance Metrics (Grass, Midday Hours)

During midday hours from 11:50 to 13:50, the ABM models estimate WBGT significantly more accurately than the Stull & BGR models, as shown by lower MAE and RMSE values (Figure 4.9). The ABM method's mean MAE values of 3.3° F (COOP data) and 3.1° F (KCUB data) outperforms the Stull & BGR models, which underpredict WBGT significantly, with mean MAEs of 4° F (COOP data) and 4.4° F (KCUB data). P-

values below 0.05 suggest the differences between these models are significantly different, making the ABM model with KCUB data the most optimal model from 11:50 to 13:50. However, this is the only situation in which ABM model conclusively performs with lower error than the Stull & BGR method.

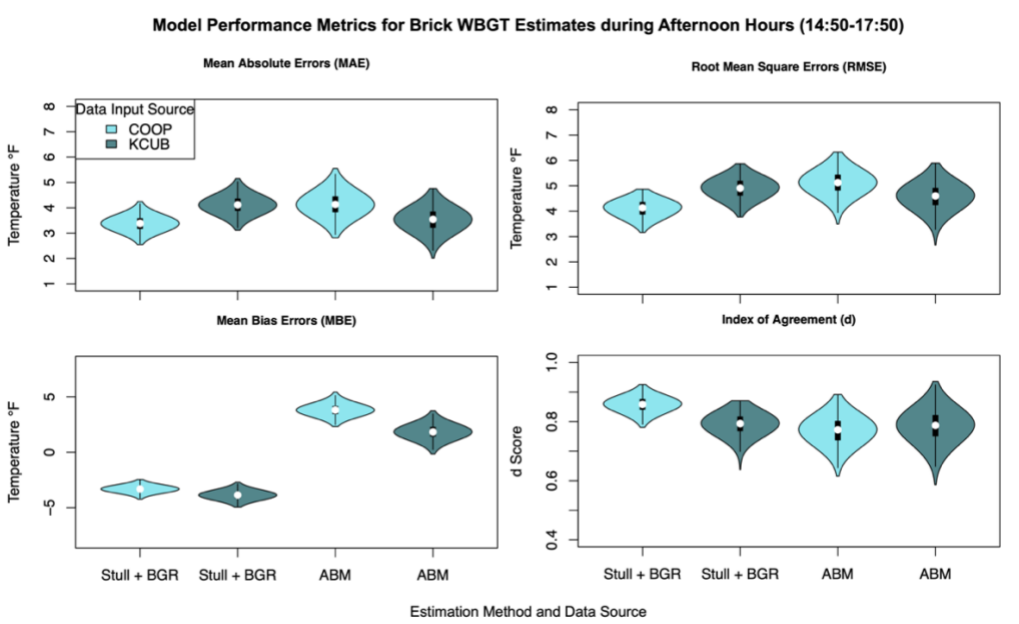

Figure 4.10 Violin Plots for Model Performance Metrics (Grass, Afternoon Hours)

Similarly, the WBGT estimation methods are rather comparable to one another during afternoon hours of 14:50 PM to 17:50 PM (Figure 3.10). The Stull & BGR (COOP data) model estimates WBGT the most accurately, with the lowest mean MAE value of 3.37 °F, and the smallest range of error (1.7 °F). This is a slight but significant improvement from the ABM (KCUB data) model, which has a mean MAE value of 3.52 °F (Table 4.1). These values suggest that the Stull & BGR using local data is the most optimal method for estimating WBGT from hours 14:50 to 17:50.

Prior to the evaluation of the Stull & BGR and ABM methods, it was desired to investigate if WBGT can be modeled using just wet and dry bulb temperatures. The

violin plots in Figure 4.11 depict 1,000 MAE, RMSE, MBE, and d index values, which help visualize the error associated with each model compared to ground truth WBGT. The model performance statistics suggests that the Wet Bulb Regression (WBR) method based on the new linear model [Equation 5] , outperformed the ABM and Stull & BGR models. The mean MAE value for the WBR model is roughly 2 °F, which indicates that this model is more accurate compared to the other four models. MBE values hover around zero which suggests that the model over and underpredicts WBGT at a similar frequency. Lastly, the WBR model has the highest d index values indicating that this proxy method agrees with WBGT more than the other four models tested in this analysis. Notably, the WBR model has d index values extraordinarily close to 1, which indicates complete model agreeance, while no other model achieves d index values this close to 1.

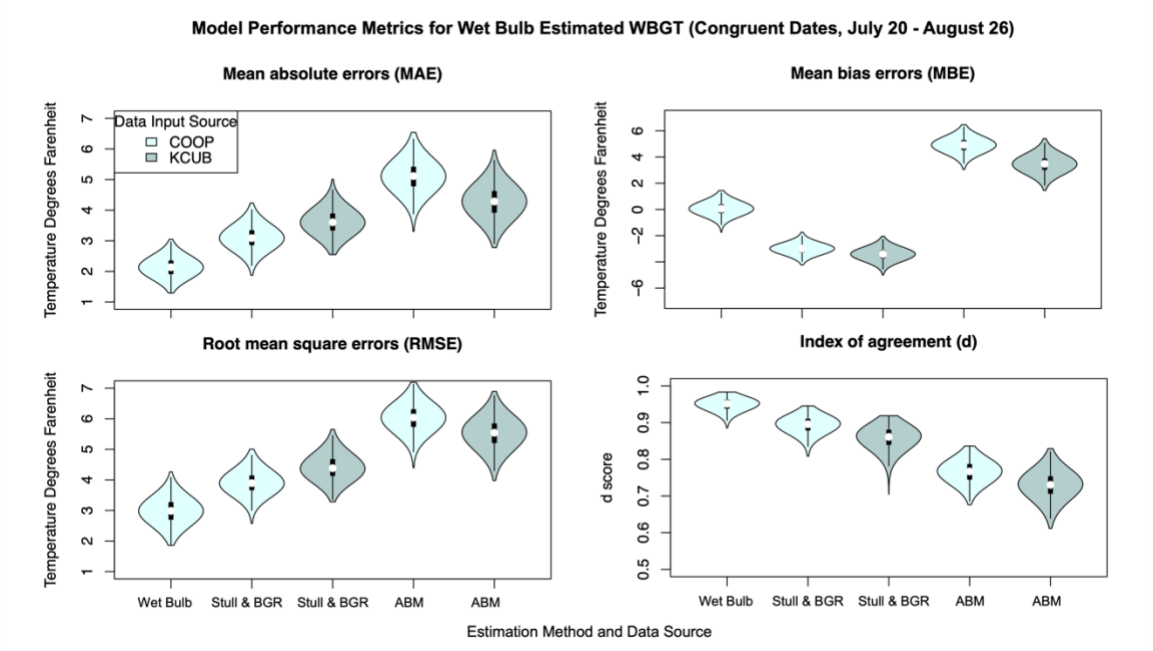

Figure 4.11 Violin Plots for Wet Bulb Regression Model Performance

4.3 LAND SURFACE ANALYSIS RESULTS

For the full data record spanning July 8 through September 23, WBGT and the variables that influence it demonstrate differential heat characteristics at the brick and grass enclaves within the COOP weather station. For all variables, grass values were subtracted from brick values. Accordingly, difference values greater than zero indicates higher values on the brick surface, and negative differences suggest higher values on the grass surface.

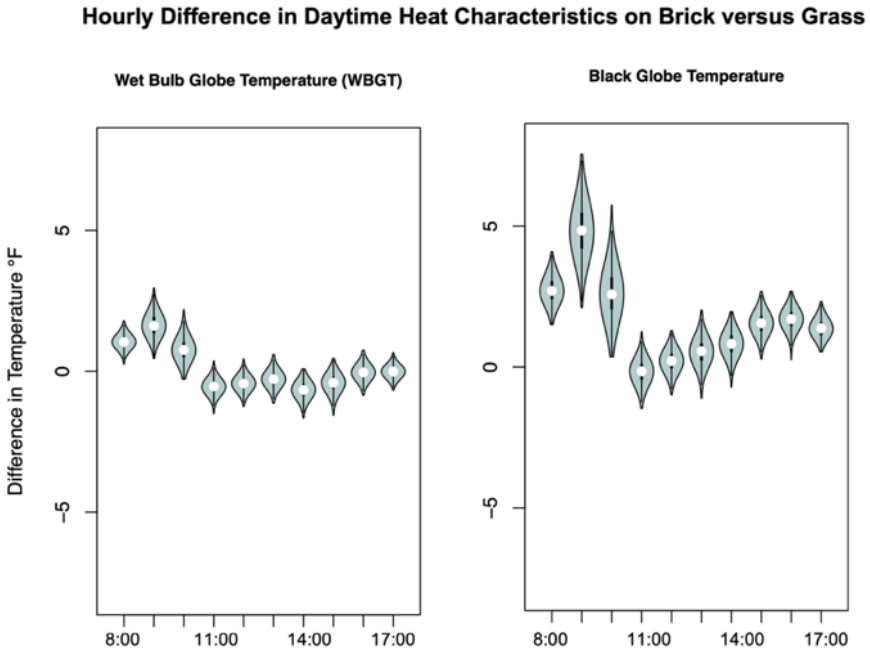

Figure 4.12 Hourly differences for WBGT and Black Globe Temperature, positive differences indicates higher values on brick

During the morning hours of roughly 8:00 to 10:00, WBGT is higher on the brick site which is made clear by the positive delta values in Figure 4.13. The reason for this is twofold. First, during these morning hours ambient temperature remains roughly 2° F warmer at the brick site. More importantly, elevated black globe temperatures are contributing to higher morning WBGT at the brick location. From 8:00 to roughly 10:00,

black globe temperature is anywhere between 2.5 °F- 6° F greater at the brick site. This noteworthy difference in black globe temperature suggests that the brick location receives more direct sunlight in the early morning. Due to its situation the brick site is likely receiving direct sunlight before the grass site does, causing higher black globe temperatures in early morning. Figure 4.13 displays solar radiation values recorded by the pyranometer at the grass site on a morning characterized by clear sky conditions. From 7:00 to approximately 9:45, solar radiation over the grass site remains below 150 W/m^2. Just before 10:00, solar radiation values dramatically spike to roughly 400 W/m^2 , and climb over the next hour until reaching nearly 700 W/m^2 at 11:00. Since black globe temperature at the brick site peaks at 9:00, and solar radiation values over grass do not drastically rise until 9:45, this indicates a slight lag in solar at the grass site. Additionally, roughly 11:00 when solar peaks at the grass site is precisely when black globe temperature delta values become closer to zero (Figure 4.13). This provides further verification that the grass location is receiving direct sunlight slightly later in the morning than the brick site.

During the midday hours from roughly 11:00 to 14:00, the difference in black globe temperature between the two sites is less stark, as the delta values hover close to zero (Figure 4.12). Since this timeframe coincides with solar noon, the two sites are receiving more even amounts of solar radiation, because the sun is at a higher angle in the sky, compared to much lower in the sky during the morning hours.

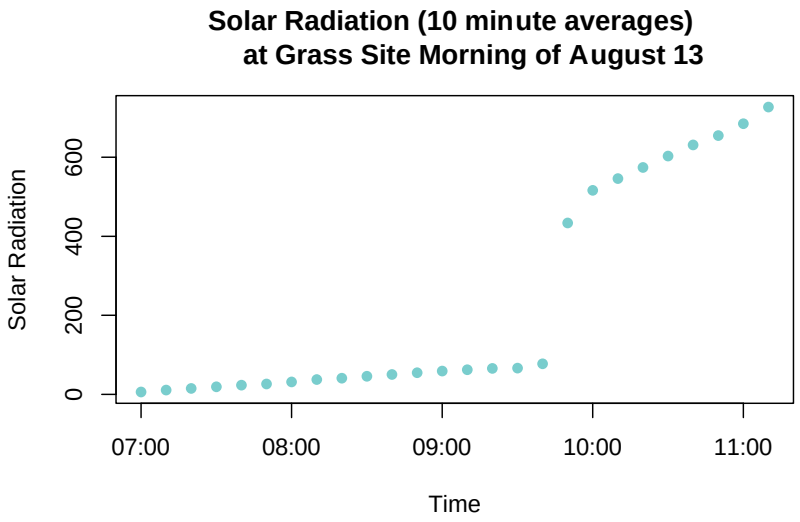

Figure 4.13 Morning Solar Radiation at the Grass COOP location

During midday and afternoon hours of approximately 11:00 to 18:00, the grass site exhibits higher WBGT values than the brick surface. This is likely attributable to WBGT subcomponents changing at the grass site during these hours. While black globe temperature remains slightly elevated on brick throughout the day, air temperature and moisture characteristics rise dramatically over the grass site during the daytime. Relative humidity remains steadily higher at the grass site, on the order of 5 to 8% (Figure 4.14), with dew point temperatures spiking between 1°- 4° F on the grass site. Similarly the wet bulb temperature remains elevated over grass from 11:00 to 18:00, anywhere from 1° - 3° F, suggesting the presence of higher air moisture at the grass location. Additionally, wind speeds are up to 1 mph faster at the brick site (Figure 4.14), indicating a slight lack of natural ventilation on the grass site. Ultimately, the interplay of elevated ambient temperature, higher moisture characteristics, and slightly slower wind speed over the grass site may help explain why WBGT is elevated there during midday and afternoon hours of 11:00 to 18:00.

These findings suggest that these variations in temporal heat characteristics may be primarily driven by the physical structure of the brick and grass microclimates themselves, rather than their respective surface types. Since the grass surface is enclosed by tree cover, compared to the open landscape of the adjacent brick measurement site, it is possible that the slower wind speeds on the grass site are leading to more stagnant air. This lack of ventilation on the grass site is congruent with the elevated wet bulb temperatures and dew points (Figure 4.14), which suggests higher water vapor content on the grass site, thus leading to higher WBGT values compared to the brick surface.

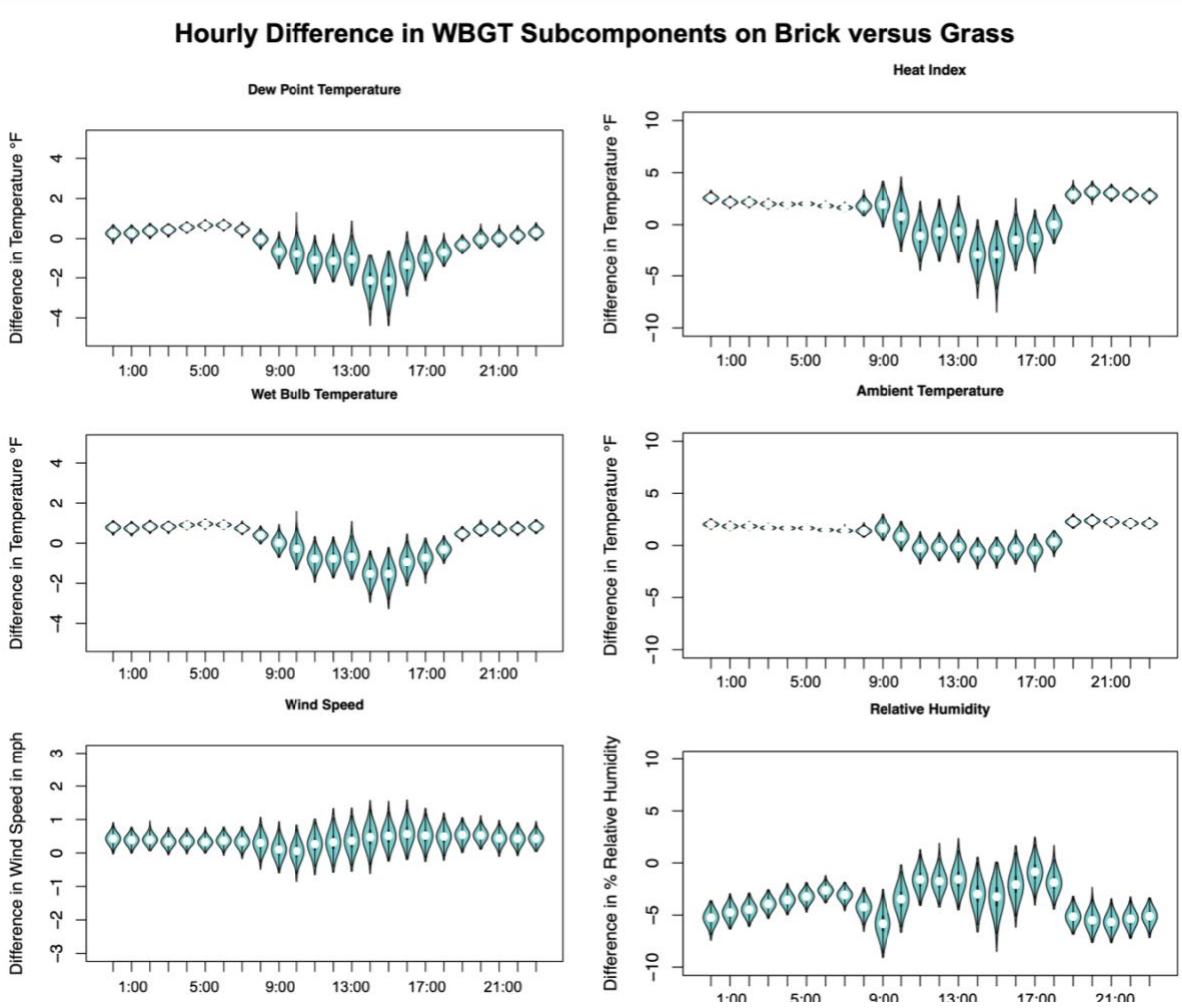

Figure 4.14 Hourly Difference on Brick versus Grass for 24 Hour Record, positive differences indicates greater values on brick

While the grass site tends to become a hotter environment during daytime hours, the brick site appears to be characterized by higher nighttime and early morning heat. Notably, both heat index and ambient temperature remain elevated over the brick surfaces during late evening hours beginning 20:00 through 8:00 the next morning. During this period, both heat index and ambient temperature values were roughly 2-3° F higher on the brick surface than on grass. Dew point and wet bulb temperatures appear slightly greater on brick, but by no more than 1° F (Figure 4.14). As stated previously, relative humidity is rarely higher over the brick site, so the elevated nighttime heat index at the brick site is likely attributed to the higher ambient temperature there, rather than moisture characteristics. In the hours of 8:00 to 10:00, nighttime heat over the brick surface continues to persist into the morning hours, and when combined with more direct sun exposure, contributes to higher morning WBGT at the brick site. Clearly, these two measurement sites experience stark diurnal changes in heat characteristics, which is a function of not only surface type, but the physical structure of each measurement area.

CHAPTER 5

DISCUSSION AND CONCLUSIONS

5.1 IMPLICATIONS FOR WBGT ESTIMATES

The intent of this research was to evaluate the effectiveness of established WBGT estimation methods and investigate if they may be reasonable substitutes for traditional instrumentation in outdoor work and sport settings. The ABM method, and the Stull & BGR models provided two different ways of estimating the full WBGT parameter using more common meteorological variables. Two distinct data sources were used as input data, to determine if proximity to WBGT recording site improves model performance.

The suite of model performance metrics indicates that on both grass and brick surfaces over the full data record, the combined Stull & BGR model estimated WBGT more accurately than the ABM method, which is made clear by lower MAE and RMSE values, as well as smaller ranges of error. This trend is rather consistent throughout the various subsets of data during different weather conditions and daily timescales, with a few exceptions. During fair weather, the ABM model performed in a manner comparable to the Stull & BGR models. The Stull & BGR model (COOP data) and ABM (KCUB data) both had mean MAE values of roughly 3.6 °F. Despite these mean MAE values being statistically indistinguishable, the Stull & BGR models had smaller error ranges suggesting this model may be more optimal than the ABM method if local data are available. Additionally, during cloud and rain conditions both Stull & BGR models significantly outperformed ABM models, which overestimated WBGT by up to 7.5° F.

This mischaracterization of WBGT during periods of heavy cloud cover and rain is expected, as the ABM model's assumption of full sun exposure is not met under such conditions. Accordingly, the ABM method (regardless of data source used) should be avoided during cloudy and rainy conditions, as the Stull & BGR model using COOP predicts WBGT with much lower error.

Similar results are exhibited for WBGT estimates during morning hours of 7:50 to 10:50. In the early morning, the Stull & BGR model estimates WBGT with lower error than both ABM models. When local COOP data are used to calculate the Stull & BGR estimates, mean MAE is lowered to 1.8° F, a significant improvement from mean MAE of 2.2° F when KCUB data are used. Like during cloudy and rainy conditions, ABM tends to significantly overestimate WBGT by a maximum of 7.8° F, as its assumption of full sunlight is questionable during morning hours characterized by low sun angle. Midday estimates from 10:50 to 13:50 are the only situation in which ABM outperformed the Stull & BGR models. The ABM model using KCUB data was characterized by the most optimal MAE value of 3.07° F, which is significantly lower than all other estimation methods. This is likely due to the assumption of full sunlight being met because this timeframe coincides with solar noon. Finally, during afternoon hours the Stull & BGR (COOP data) and ABM (KCUB) models were characterized by mean MAE values of 3.37° F and 3.5° F, respectively. There was no significant difference between the mean MAE of the two models, suggesting that the Stull & BGR model performs slightly better than the ABM, but this improvement is non-significant. During these hours of 14:50 to 17:50, the ABM models still overestimate WBGT, but by not nearly as much as during morning hours and during cloudy conditions. Similar to the midday hours, the

underlying assumptions of the ABM method are likely met in this scenario during afternoon hours of direct sunlight. However, since the range of error is much smaller for the Stull & BGR model, this is likely preferred over the ABM method, which has a more spread out error range, suggesting the ABM method is more erratic in nature.

Results from this analysis demonstrate that the use of meteorological inputs from different data sources had a significant impact on WBGT estimation error. The use of localized COOP data dramatically improved the Stull & BGR estimated WBGT, while the ABM model actually performed more optimally when KCUB airport data were used. Originally, it was hypothesized that the use of localized data, as opposed to airport data, would improve all the WBGT estimates. Further evaluation is required to determine why the ABM method performs less accurate with in-situ data, and if this phenomena is locally specific.

Under all scenarios, the ABM model conservatively overestimated WBGT, while the Stull & BGR method consistently underpredicted true values. In practice this means that use of the ABM model would likely curtail work and sport more frequently, erring on the side of caution regarding potential heat casualties. In real world work and sport settings where the ABM method is used to monitor WBGT, the opportunity costs of missed work and practice time should be considered. Alternatively, the Stull & BGR models underprediction of WBGT would translate into slightly more liberal observations, which may give a false indication that outdoor conditions are safer than they actually are.

It should be noted that in practice, the model errors identified in this research could be large enough to jump WBGT flag categories. Figures 5.1 – 5.3 depict flag categories associated with observed WBGT, compared to predicted values from the three

models. For example, the ABM (KCUB data) model has a mean MAE value of 4.28° F under all conditions, which is a large enough error to initiate black flag status (90°F), when the actual conditions are characterized by the more mild yellow flag status (Figure 1.1). Figure 5.1 shows the frequency at which the ABM method tends to overestimate observed WBGT values. Many observed WBGT values in the green flag category (80-85°F) are overestimated and designated in yellow, red, and black flag categories. This mischaracterization of heat exposure would cause false alarms where work would be curtailed unnecessarily, thus causing lost work and practice time.

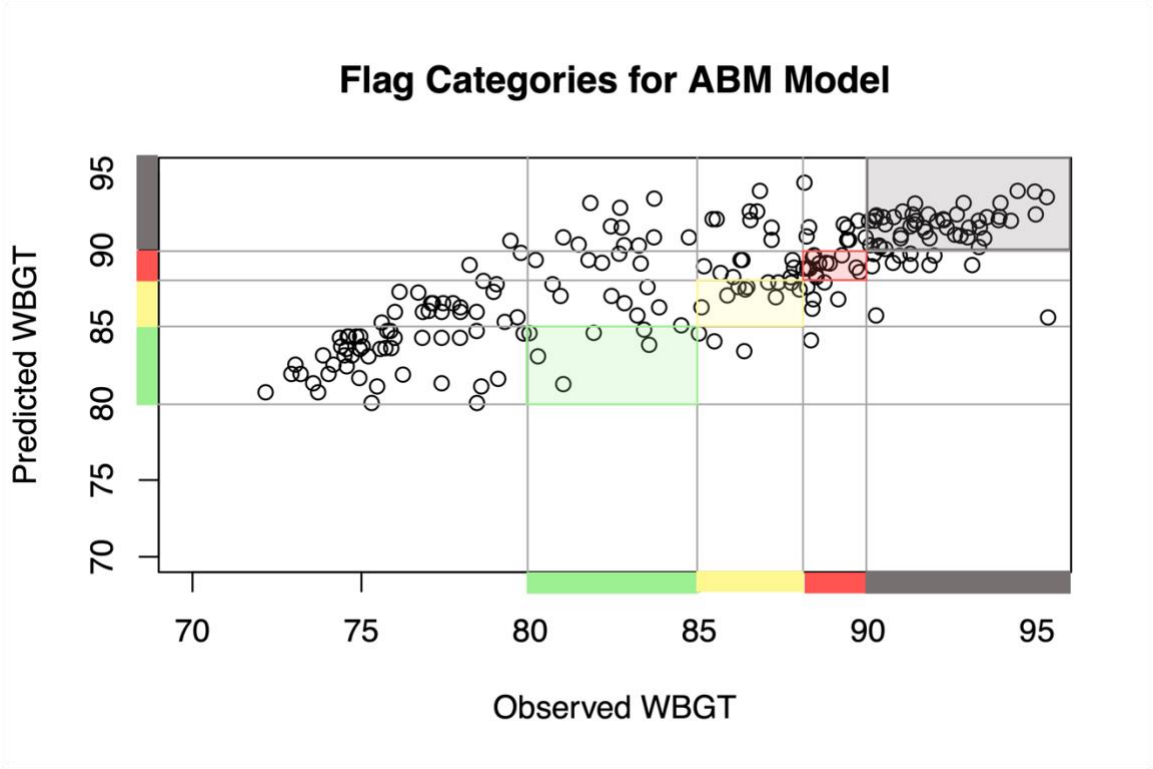

Figure 5.1 Flag Categories for Observed and Predicted WBGT values (ABM, KCUB data)

The general trend of overestimation of ABM model, especially during morning hours and cloudy or rainy weather conditions, is consistent with the original hypothesis and prior literature. Several other researchers have evaluated the magnitude of error

associated with the ABM method. A study in Georgia (Grundstein & Cooper, 2018) compared ABM estimation against the Liljegren WBGT model, which was held as the direct observation for comparison purposes. In this study the ABM model generally overestimated WBGT, especially during morning and evening hours, and was most accurate between 10:00 am to 2:00 pm. A similar evaluation sought to compare on site WBGT measurements against WBGT estimates from a mobile app that used the ABM model as its theoretical basis. (Tripp et al., 2020). Analyses of the two metrics reflected similar results, in which the ABM approximations tended to overestimate WBGT, and such deviations were particularly stark in the late afternoon hours with low sun angle. Alternatively, other analyses have identified (Teimori et al., 2020) significant positive relationships between ABM estimates and true WBGT, with highest correlation coefficients at noon (0.931), followed by 9:00 am (0.905), and 5:00 pm (0.875). However, correlations tend to do a poor job at assessing observed versus modeled variances, so this analysis may be less reliable than others.

Alternatively, while the Stull & BGR models tend to have lower magnitude of error than the ABM method, WBGT flag categories are often mischaracterized. For example, during midday hours from 11:50 to 13:50, the Stull & BGR models error more than in any other scenario. When using local COOP data during these midday hours, this model underestimated WBGT by an average of 4.04° F, which could theoretically misconstrue black flag conditions (90° F) as yellow flag conditions (86°F). Figure 5.2 depicts observed and predicted WBGT values for this model. Clearly, many observed WBGT values in the black flag category (90°F or greater) are underpredicted and characterized as yellow and red flag status. Accordingly, while the Stull & BGR method

generally performs better than ABM models, the use of this estimation method would likely result in an underprediction of heat exposure in most scenarios.

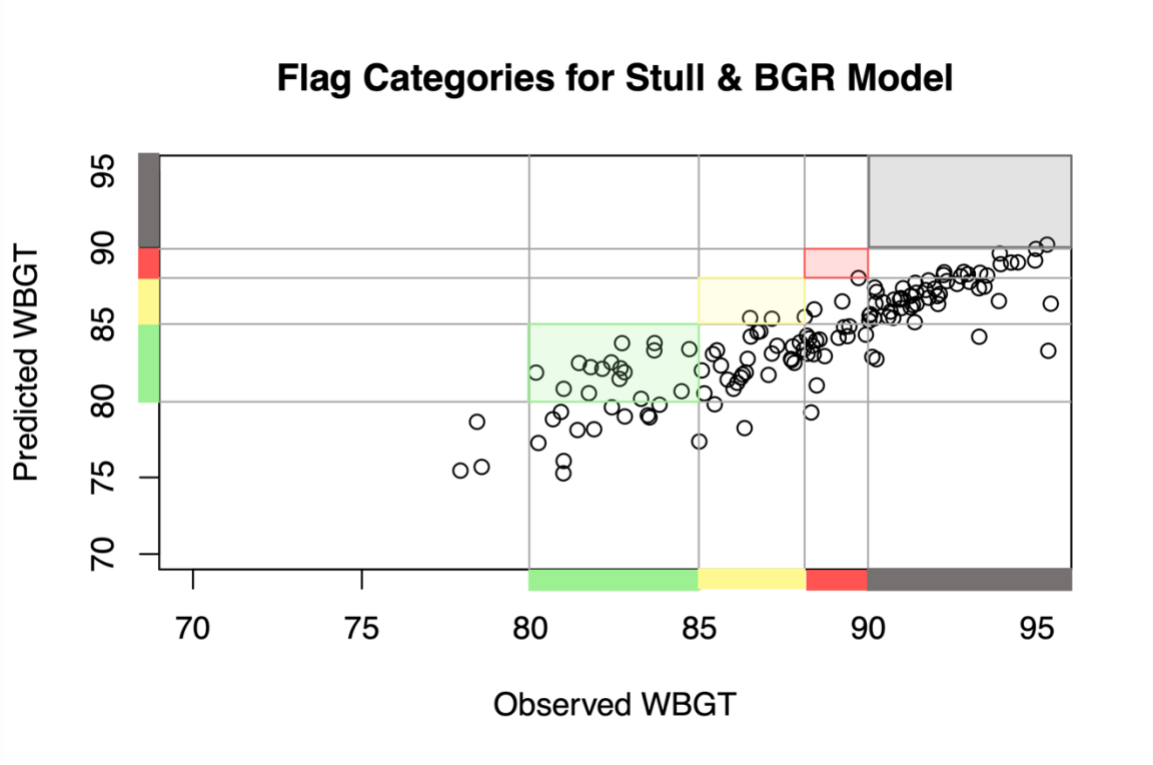

Figure 5.2 Flag Categories for Observed and Predicted WBGT values (Stull & BGR, COOP data)

Surprisingly, the simplest model (using only wet-bulb temperature performs better than the ABM and Stull & BGR methods, as measured by MAE, RMSE, and d index values. Despite its lower error, this method still can mischaracterize WBGT flag status (Figure 5.3). While many black flag measurements are properly characterized, the WBR model dramatically underestimates WBGT values above 90°F in some cases, which could underestimate heat exposure risk. Additionally, many observed green flag measurements are overpredicted when using the WBR method, which could lead to the curtailment of outdoor work.

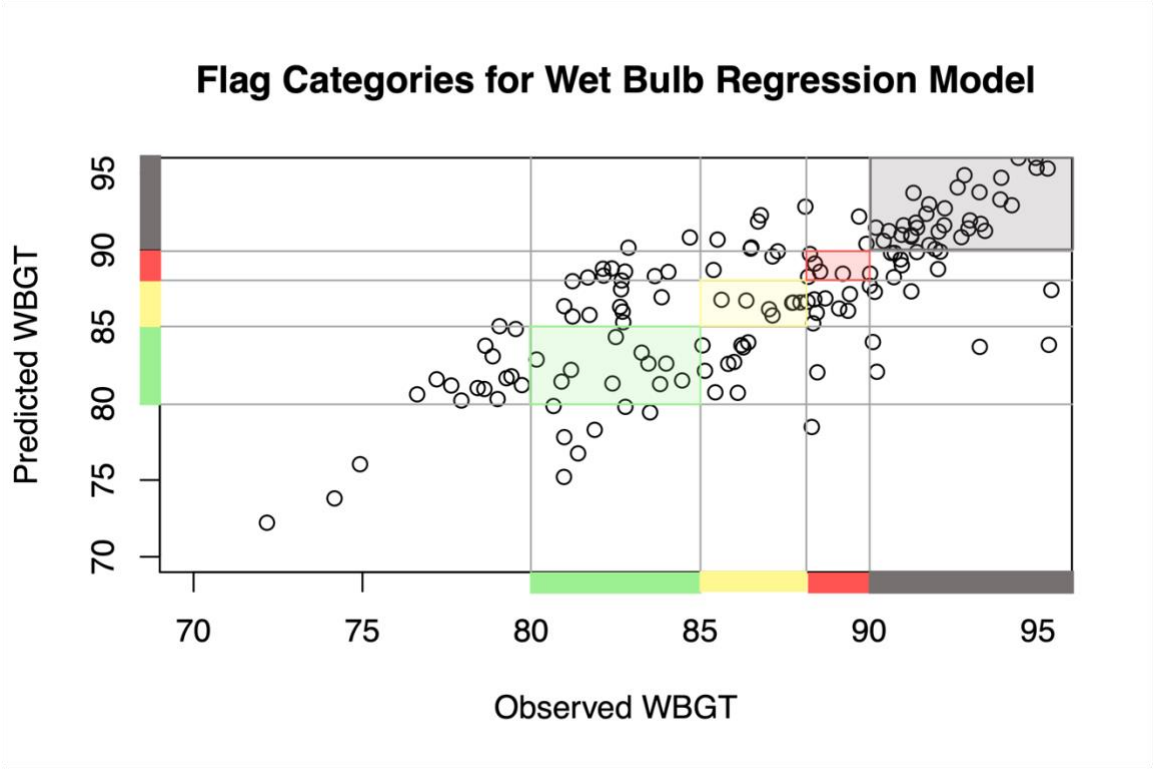

Figure 5.3 Flag Categories for Observed and Predicted WBGT values (WBR, COOP data)

Despite its tendency to misrepresent flag categories at times, the WBR method may serve as a promising method for estimating WBGT that warrants further investigation. Since the two inputs, wet bulb and dry bulb temperatures, can be measured at little cost and with relative ease using a sling psychrometer, this method could make WBGT monitoring accessible to a wide swath of the population. Additionally, by using a sling psychrometer to approximate WBGT at a sports practice field or outdoor worksite, locally specific heat characteristics will be considered, as opposed to using data from the nearest ASOS station. Further analysis should explore the conditions and times of day in which this model performs the least optimally, and attempt to ameliorate these errors.

In summary, the ABM model using airport data inputs may be suitable during fair weather conditions and hours close to solar noon, but still overpredicts WBGT by several degrees. Although this model leans rather conservative regarding the regulation of human heat exposure, it will likely cause unnecessary curtailment of work, especially in climates that experience frequent precipitation and cloud cover. Thus, Columbia, SC experiences consistent rainfall year-round, making this location potentially less suitable for use of the ABM model. In comparison, the ABM model may be more amenable in semi-arid or arid desert cities that experience consistent elevated solar radiation and limited annual precipitation. During all other situations, the Stull & BGR method using a localized data source is the more optimal choice for estimating WBGT, as demonstrated by its relatively low errors compared to ABM, especially during periods of heavy cloud cover and early morning hours. This finding is congruent with the original hypothesis, as the Stull & BGR method integrates solar radiation as an input variable and is thus slightly more sophisticated than the ABM model. However, it should be noted that in most cases, this method will underestimate heat risk, which could result in heat casualties. In reaction to these drawbacks, a preliminary analysis suggests that predicting WBGT using dry and wet bulb temperatures may serve as a more accurate proxy method characterized by lower errors.

5.2 IMPLICATIONS FOR LAND USE ANALYSIS

The second goal of this study was to explore how WBGT and its subcomponents vary across a grass and brick surface, and to understand diurnal fluctuations in heat characteristics. Differences between ambient temperature and heat index on the two sites demonstrated very similar trends over the 24 hour period, with elevated values at the

brick site at nighttime and early morning hours, and higher values at the grass surface during the day. WBGT values were higher over brick during early morning hours from roughly 8:00 to 10:00, but remained elevated over the grass for the majority of daylight hours.

It is believed that the elevated heat at the grass site during the daytime, including both WBGT and heat index, is likely caused by higher moisture characteristics in this area. First, percent relative humidity remains consistently higher at the grass site for the entire 24-hour period, even as the air temperature there increases during afternoon hours. Normally, it is expected that relative humidity will decrease as daily temperature increases. So, the consistent pattern of elevated humidity levels on the grass site may be indicative of higher moisture levels in this area, rather than just diurnal fluctuations in temperature. Figure 4.14 clearly demonstrates elevated dew point temperatures and wet bulb temperatures at the grass site, indicating higher air moisture levels there. This may be caused by several factors. First, since the grass measurement site is encircled by thick tree cover (but the Kestrel instrument was in direct sunlight) it is possible that increased shade cover surrounding the grass site may inhibit evaporation of water and keep moisture levels higher, compared to the brick measurement site which has virtually no surrounding shade cover. Additionally, since the grass site is enclosed by trees on three sides (compared to the relatively open nature of the brick measurement site) it is possible that stagnant air is staying confined within the site, contributing to higher moisture levels on grass. In addition to the higher dew point temperatures on grass, the interplay of wind speed and wet bulb temperature may help to further explain elevated heat characteristics at the grass site. Wind speeds appear to be slightly lower on the grass site, suggesting this

area gets less air ventilation compared to the brick surface. Since faster wind speeds can facilitate the evaporation of water, this helps explain why wet bulb temperatures are up to 3° F higher on the grass surface. Alternatively, the slightly faster moving wind speeds on the brick site may serve as a mechanism to move water vapor away, which is keeping wet bulb temperatures lower at this area. Accordingly, it is theorized that the daytime heat characteristics within the grass site may be more related to the physical structure of the site, rather than solely the type of land surface.

Alternatively, the higher nighttime temperatures on the brick site are likely a function of higher specific heat capacity of the brick versus grass surface. This pattern is congruent with the way in which urban metropolitan areas tend to be several degrees warmer compared to their rural counterparts. Due to increased built surfaces that traps solar radiation, this trend on the brick surface exemplifies the urban heat island (UHI) effect at a smaller scale. The UHI is characterized by higher nighttime minimum temperatures, which has become an area of concern because elevated minimum temperatures deprives the human body an opportunity to cool down and physiologically recover from daytime heat exposure (Habeeb et al., 2015). Accordingly, the trend of heightened nighttime temperature and heat index values over the brick surface conforms to the pattern of urban built environment, which exacerbates nighttime heat in summer months.

Heat characteristics persisted into nighttime hours likely due to the greater heat capacity of the brick surface, but the morning heat conditions at this site appear more so related to the microclimate structure itself. It is believed that elevated morning WBGT over the brick site is largely a function of higher air temperature and black globe

temperature values. Due to its location and position rather than land surface type, the brick site was able to receive solar radiation earlier in the morning than the grass site, which caused heightened WBGT from 8:00 to roughly 10:00. Ultimately, this difference in solar radiation across these two sites reinforces the usefulness of WBGT as a monitoring tool. Other metrics such as temperature or heat index would fail to capture the effects of sunlight, which in this particular case, appear to vary across the small geographic vicinity of the COOP site.

The results from this land surface analysis demonstrates how WBGT, and the components that influence it, can vary across both microclimate and time of day. Accordingly, difference measures can be situated in the context of the WBGT estimation error from this analysis. For example, WBGT and ambient temperature can vary up to 1° F on the brick versus grass surface during the day. Accordingly, mean MAE values for the full data record for Stull & BGR model (COOP data) were 3.12° F on grass, and 2.91 °F on brick. In this particular example, the difference in average model error is less than the difference in WBGT between the two surfaces. The same is true for ABM estimated COOP, which over the 1 month record had mean MAE values of 5.12°F on grass, and 5.15° F on the brick surface. This suggests that the difference in model error across the two measurement sites is smaller than the delta value for observed WBGT, and error is likely associated with the models themselves rather than specific location.

These findings may present useful recommendations for building and planning purposes. The enhanced moisture levels and inhibited wind speeds within the grass enclave demonstrates the need for designing urban landscapes with some open spaces, to allow air to move more freely. While the tree cover surrounding the grass site

demonstrates how vegetation may block wind and serve as a mechanisms for trapping air moisture, the vegetation also allowed this site to cool down at nighttime. At nighttime, air temperatures and heat index values remained elevated over the brick surface and persisted into early morning hours, suggesting the need for vegetation cover to serve as a nighttime cooling mechanism. Further investigation is needed to determine the proper balance between taking advantage of the cooling benefits of vegetation cover, while also promoting air movement within cities and urban environments. Also, the spikes in daytime WBGT and heat index over grass during the daytime demonstrates the importance of increasing air ventilation as a humidity reduction strategy. Since wet bulb temperature is the heaviest weighted component of WBGT, it is clear through these associations that humidity has a noteworthy impact on WBGT, and therefore outdoor heat safety.

5.3 LIMITATIONS

Data gaps pose a hindrance to this research. Missing data, both from variables recorded at the COOP and airport sites, resulted in the inability to estimate WBGT during those times. Ultimately, this diminished the final number of predicted versus observed WBGT datapoints available for analysis. However, the statistical power of the record remained robust. Additionally, the anemometer for measuring wind speed did not arrive until the first week of August, and the pyranometer stopped recorded solar radiation data just two weeks afterwards. Accordingly, all four atmospheric variables that make up WBGT (temperature, humidity, wind, and solar), were only available over congruent times for less than a two-week period. Lastly, it was not possible to obtain solar radiation off site, so the KCUB Stull & BGR model was calculated using airport temperature and

humidity, but solar radiation measured at the COOP site. It would have been preferable to evaluate the impact of off-site solar radiation on WBGT model performance, especially since solar radiation is likely not feasible to measure at a common workplace or school.

It was originally intended to calculate the previously mentioned WBGT estimates in the Charleston, SC study area. The nature of the study design in Charleston provided an opportunity to evaluate how these estimates may perform at various efficacies across a variety of land surfaces and microclimates, which was not a possibility in the Columbia study. However, the sampling across roughly ten microclimate locations in downtown Charleston severely hindered the record of data that could feasibly be collected. Due to the study design, each microclimate location only had several hours' worth of WBGT measurements, which if aggregated up to an hourly timestamp in accordance with airport data, would not provide enough data points to ensure statistical power. Accordingly, it was not feasible to model WBGT in Charleston for this dataset, as more datapoints would be needed to establish any meaningful or robust conclusions. Additionally, it should be noted that the data collection for this analysis took place during a summer that was not as hot compared to more recent years in the state of South Carolina. The highest maximum temperature during Summer 2021 recorded at the USC COOP station was 98° F, on August 27th. This can be compared to the record breaking 113° F temperature observation at USC Columbia COOP site in 2012.

Finally, the land surface analysis was limited somewhat by design. Due to the expensive instrumentation costs, it was important to situate the Kestrels in a secured area where they would not be stolen or tampered with. Thus, the Kestrels were situated at the secured COOP weather station. Many desirable measurement locations, such as asphalt

or concrete surfaces, would have served as interesting comparisons for this study, but were sacrificed to protect the instruments.

5.4 CONCLUSIONS

The societal and public health ramifications of extreme heat are well documented by a variety of epidemiological, climatological, and geographic research. The synthesis of this research suggests potential for exacerbated morbidity and mortality events induced by heat wave events and periods of elevated temperatures that can be expected as society moves forward in a changing climate. Given the threat of rising global temperatures to both human health and economic productivity, proper understanding and monitoring of environmental heat hazards is essential in the coming decades. Accordingly, honing proxy methods for metrics like WBGT is a potential avenue for adapting to a changing climate by effectively monitoring and discouraging outdoor activity during unsafe heat conditions.

Based on results of this study, it is believed that using the Stull equation for wet bulb temperature, and modeling black globe temperature using solar radiation values and temperature is preferable to the ABM method for estimating WBGT, if data inputs within or near the work site are available. Despite the Stull & BGR methods lower error compared to ABM, it is not without fault. Due to its consistent underestimation, this method could misconstrue heat exposure, and allow outdoor activity during times when it is dangerous. It was discovered that calculating WBGT using this model with localized data improves model performance compared to free, publicly available weather station data. However while this methods may be sound proxy method for WBGT in some cases, measuring the necessary variables is likely not feasible at many sites. While the ABM

model has a tendency to estimate WBGT less accurately, it has the advantage of only requiring temperature and relative humidity, which is publicly available to any worksite supervisor or athletic coach. Additionally, the ABM method performs more accurately when airport data are used, versus onsite measurements, making it a much more practical option for the general public. Building off of these findings, it was determined that a linear model can reasonably predict WBGT using dry and wet bulb temperature components, which can be measured using a sling psychrometer. The WBR model (Figure 4.11) tended to outperform the ABM and Stull & BGR methods, suggesting that this may be a more accurate, and simple way to estimate WBGT. Since more data were needed to evaluate WBGT estimates in various urban settings in Charleston, SC, future research is needed to evaluate how transferrable these results are across space.

Lastly, the land surface results in this analysis further reinforce the notion that heat exposure is influenced by an array of variables, with land surface type being just one factor. Across a small geographic vicinity in the COOP site, stark differences in heat characteristics such as humidity levels, solar radiation, and even ambient temperature were present. Originally it was envisioned to understand how heat varies in response to the two land surface types represented here, with all other factors being held equal. However the assumption that the two measurement sites were completely identical (other than their surface types) was not met. Differences in the structure of the brick and grass sites created distinct microclimates that manifested into hotter daytime heat over the grass surface caused by stagnant air and moisture laden conditions, and elevated nighttime temperatures at the brick site due to its higher heat capacity. Ultimately, these findings

suggest a need to further evaluate the influence of microclimate structure on heat exposure for building and planning purposes.

In response to recent and unprecedented heatwave events in the Pacific Northwest Region, as well as the current administration's efforts to prioritize heat safety at American worksites via OSHA guidelines, monitoring and understanding outdoor heat has become a critical area of concern in the context of public health and climate adaptation. Accordingly, while the WBGT estimates explored in this analysis may be useful in certain scenarios, these methods are still flawed and have the potential to mischaracterize heat exposure. In response, further work should be prioritized in order to better understand how heat manifests differently across time and space, and to hone effective proxy methods to make WBGT monitoring accessible to all stakeholders.

REFERENCES

Allen, R. G., Pereira, L. S., Raes, D., & Smith, M. (1998). FAO Irrigation and Drainage Paper No.56 Crop Evapotranspiration. Rome, Italy: Food and agriculture Organization of the United Nations.

American College of Sports Medicine. (1984). *Prevention of Thermal Injuries During Distance Running, Position Stand*.

Australian Bureau of Meteorology. (2010). *Thermal Comfort observations.* Australian Government
Bureau of Meteorology, Weather Services.
http://www.bom.gov.au/info/thermal_stress/#approximation

Bailey, E., Fuhrmann, C., Runkle, J., Stevens, S., Brown, M., & Sugg, M. (2020). Wearable sensors for personal temperature exposure assessments: A comparative study. *Environmental Research*, *180*, 108858. https://doi.org/10.1016/j.envres.2019.108858

Bekkar, B., Pacheco, S., Basu, R., & DeNicola, N. (2020). Association of Air Pollution and Heat Exposure With Preterm Birth, Low Birth Weight, and Stillbirth in the US: A Systematic Review. *JAMA Network Open*, *3*(6), e208243. https://doi.org/10.1001/jamanetworkopen.2020.8243

Budd, G. M. (2008). Wet-bulb globe temperature (WBGT)—Its history and its limitations. *Journal of Science and Medicine in Sport*, *11*(1), 20–32. https://doi.org/10.1016/j.jsams.2007.07.003

Carter, A. W., Zaitchik, B. F., Gohlke, J. M., Wang, S., & Richardson, M. B. (2020). Methods for Estimating Wet Bulb Globe Temperature From Remote and Low-Cost Data: A Comparative Study in Central Alabama. *GeoHealth*, *4*(5). https://doi.org/10.1029/2019GH000231

Carter, L. M., Terando, A., Dow, K., Hiers, K., Kunkel, K. E., Lascurain, A., Marcy, D. C., Osland, M. J., & Schramm, P. J. (2018). *Chapter 19: Southeast. Impacts, Risks, and Adaptation in the United States: The Fourth National Climate Assessment, Volume II*. U.S. Global Change Research Program. https://doi.org/10.7930/NCA4.2018.CH19

Cooper, E., Grundstein, A., Rosen, A., Miles, J., Ko, J., & Curry, P. (2017). An Evaluation of Portable Wet Bulb Globe Temperature Monitor Accuracy. *Journal of Athletic Training*, *52*(12), 1161–1167. https://doi.org/10.4085/1062-6050-52.12.18

Dimiceli, V. E., Piltz, S. F., & Amburn, S. A. (2011). *Estimation of Black Globe Temperature for Calculation of the Wet Bulb Globe Temperature Index*. 9.

Ebi, K. L., Balbus, J., Luber, G., Bole, A., Crimmins, A. R., Glass, G. E., Saha, S., Shimamoto, M. M., Trtanj, J. M., & White-Newsome, J. L. (2018). *Chapter 14: Human Health. Impacts, Risks, and Adaptation in the United States: The Fourth National Climate Assessment, Volume II*. U.S. Global Change Research Program. https://doi.org/10.7930/NCA4.2018.CH14

Fryar, C. D. (2012). *Prevalence of Uncontrolled Risk Factors for Cardiovascular Disease: United States, 1999–2010*. *103*, 8.

Fuhrmann, C. M., Sugg, M. M., Konrad, C. E., & Waller, A. (2016). Impact of Extreme Heat Events on Emergency Department Visits in North Carolina (2007–2011). *Journal of Community Health*, *41*(1), 146–156. https://doi.org/10.1007/s10900-015-0080-7

Greenberg, J. H., Bromberg, J., Reed, C. M., Gustafson, T. L., & Beauchamp, R. A. (1983). The epidemiology of heat-related deaths, Texas—1950, 1970-79, and 1980. *American Journal of Public Health*, *73*(7), 805–807. https://doi.org/10.2105/AJPH.73.7.805

Grundstein, A., & Cooper, E. (2018). Assessment of the Australian Bureau of Meteorology wet bulb globe temperature model using weather station data. *International Journal of Biometeorology*, *62*(12), 2205–2213. https://doi.org/10.1007/s00484-018-1624-1

Grundstein, A. J., Hosokawa, Y., & Casa, D. J. (2018). Fatal Exertional Heat Stroke and American Football Players: The Need for Regional Heat-Safety Guidelines. *Journal of Athletic Training*, *53*(1), 43–50. https://doi.org/10.4085/1062-6050-445-16

Grundstein, A., Williams, C., Phan, M., & Cooper, E. (2015). Regional heat safety thresholds for athletics in the contiguous United States. *Applied Geography*, *56*, 55–60. https://doi.org/10.1016/j.apgeog.2014.10.014

Gubernot, D. M., Anderson, G. B., & Hunting, K. L. (2014). The epidemiology of occupational heat exposure in the United States: A review of the literature and assessment of research needs in a changing climate. *International Journal of Biometeorology*, *58*(8), 1779–1788. https://doi.org/10.1007/s00484-013-0752-x

Habeeb, D., Vargo, J., & Jr, B. S. (2015). Rising heat wave trends in large US cities. *Nat Hazards*, 15.

Hajizadeh, R., Farhang Dehghan, S., Golbabaei, F., Jafari, S. M., & Karajizadeh, M. (2017). Offering a model for estimating black globe temperature according to meteorological measurements: A model for estimating black globe temperature. *Meteorological Applications*, *24*(2), 303–307. https://doi.org/10.1002/met.1631

Kalkstein, L. S., & Davis, R. E. (1989). Weather and Human Mortality: An Evaluation of Demographic and Interregional Responses in the United States. *Annals of the*

Association of American Geographers, *79*(1), 44–64. https://doi.org/10.1111/j.1467-8306.1989.tb00249.x

Kenney, W. L., Craighead, D. H., & Alexander, L. M. (2014). Heat Waves, Aging, and Human Cardiovascular Health. *Medicine & Science in Sports & Exercise*, *46*(10), 1891–1899. https://doi.org/10.1249/MSS.0000000000000325

Kovach, M. M., Konrad, C. E., & Fuhrmann, C. M. (2015). Area-level risk factors for heat-related illness in rural and urban locations across North Carolina, USA. *Applied Geography*, *60*, 175–183. https://doi.org/10.1016/j.apgeog.2015.03.012

Lehmacher, E. J., Jansing, P., & Kupper, T. (2006). Thermophysiological Responses Caused by Ballistic Bullet-Proof Vests. *The Annals of Occupational Hygiene*. https://doi.org/10.1093/annhyg/mel056

Lemke, B., & Kjellstrom, T. (2012). Calculating Workplace WBGT from Meteorological Data: A Tool for Climate Change Assessment. *Industrial Health*, *50*(4), 267–278. https://doi.org/10.2486/indhealth.MS1352

Liljegren, J. C., Carhart, R. A., Lawday, P., Tschopp, S., & Sharp, R. (2008). Modeling the Wet Bulb Globe Temperature Using Standard Meteorological Measurements. *Journal of Occupational and Environmental Hygiene*, *5*(10), 645–655. https://doi.org/10.1080/15459620802310770

Luque, J. S., Bossak, B. H., Davila, C. B., & Tovar-Aguilar, J. A. (2019). "I Think the Temperature was 110 Degrees!": Work Safety Discussions Among Hispanic Farmworkers. *Journal of Agromedicine*, *24*(1), 15–25. https://doi.org/10.1080/1059924X.2018.1536572

Matthew, W., Santee, W., & Larry, B. (2001). *Solar Load Inputs for Thermal Strain Models and the Solar Radiation Sensitive Components of the WBGT Index. Technical Report T01-13.* US Army Research Institute of Environmental Medicine.

Meehl, G. A., & Tebaldi, C. (2004). *More Intense, More Frequent, and Longer Lasting Heat Waves in the 21st Century*. *305*, 5.

Mora, C., Dousset, B., Caldwell, I. R., Powell, F. E., Geronimo, R. C., Bielecki, C. R., Counsell, C. W. W., Dietrich, B. S., Johnston, E. T., Louis, L. V., Lucas, M. P., McKenzie, M. M., Shea, A. G., Tseng, H., Giambelluca, T. W., Leon, L. R., Hawkins, E., & Trauernicht, C. (2017). Global risk of deadly heat. *Nature Climate Change*, *7*(7), 501–506. https://doi.org/10.1038/nclimate3322

National Oceanic and Atmospheric Administration (NOAA). *Weather Related Fatality and Injury Statistics*. 2020. National Weather Service.

Otani, H., Goto, T., Goto, H., & Shirato, M. (2017). Time-of-day effects of exposure to solar radiation on thermoregulation during outdoor exercise in the heat. *Chronobiology International*, *34*(9), 1224–1238. https://doi.org/10.1080/07420528.2017.1358735

Patel, T., Mullen, S. P., & Santee, W. R. (2013). Comparison of Methods for Estimating Wet-Bulb Globe Temperature Index From Standard Meteorological

Measurements. *Military Medicine*, *178*(8), 926–933. https://doi.org/10.7205/MILMED-D-13-00117

Raymond, C., Matthews, T., & Horton, R. M. (2020). The emergence of heat and humidity too severe for human tolerance. *Science Advances*, *6*(19), eaaw1838. https://doi.org/10.1126/sciadv.aaw1838

Roberts, A. W., Ogunwole, S. U., Blakeslee, L., & Rabe, M. A. (n.d.). *The Population 65 Years and Older in the United States: 2016*. 25.

Semenza, J. (1999). Excess hospital admissions during the July 1995 heat wave in Chicago. *American Journal of Preventive Medicine*, *16*(4), 269–277. https://doi.org/10.1016/S0749-3797(99)00025-2

Smargiassi, A., Goldberg, M. S., Plante, C., Fournier, M., Baudouin, Y., & Kosatsky, T. (2009). Variation of daily warm season mortality as a function of micro-urban heat islands. *Journal of Epidemiology & Community Health*, *63*(8), 659–664. https://doi.org/10.1136/jech.2008.078147

Stull, R. (2011). Wet-Bulb Temperature from Relative Humidity and Air Temperature. *Journal of Applied Meteorology and Climatology*, *50*(11), 2267–2269. https://doi.org/10.1175/JAMC-D-11-0143.1

Teimori, G., Monazzam, M. R., Nassiri, P., Golbabaei, F., Dehghan, S. F., Ghannadzadeh, M. J., & Asghari, M. (2020). Applicability of the model presented by Australian Bureau of Meteorology to determine WBGT in outdoor workplaces: A case study. *Urban Climate*, *32*, 100609. https://doi.org/10.1016/j.uclim.2020.100609

Tripp, B., Vincent, H. K., Bruner, M., & Smith, M. S. (2020). Comparison of wet bulb globe temperature measured on-site vs estimated and the impact on activity modification in high school football. *International Journal of Biometeorology*, *64*(4), 593–600. https://doi.org/10.1007/s00484-019-01847-2

Ward, A., Clark, J., McLeod, J., Woodul, R., Moser, H., & Konrad, C. (2019). The impact of heat exposure on reduced gestational age in pregnant women in North Carolina, 2011–2015. *International Journal of Biometeorology*, *63*(12), 1611–1620. https://doi.org/10.1007/s00484-019-01773-3

Whitman, S., Good, G., Benbow, N., Shou, W., & Mou, S. (1997). *Mortality in Chicago Attributed to the July 1995 Heat Wave*. *87*(9), 5.

Willmott, C. J. (1982). *Some Comments on the Evaluation of Model Performance*. *63*(11), 5.

Yaglou, C., & Minard, D. (1957). Control of Heat Casualties at Military Training Centers. *Archives of Industrial. Health*.